

# Magnetic impurities in a superconductor: Effect of domain walls and interference

P. D. Sacramento,<sup>1</sup> V. K. Dugaev,<sup>1,2</sup> and V. R. Vieira<sup>1</sup>

<sup>1</sup>*Departamento de Física and CFIF, Instituto Superior Técnico, Universidade Técnica de Lisboa, Avenida Rovisco Pais, 1049-001 Lisboa, Portugal*

<sup>2</sup>*Department of Mathematics and Applied Physics, Rzeszów University of Technology, Aleja Powstańców Warszawy 6, 35-959 Rzeszów, Poland*

(Received 12 March 2007; revised manuscript received 2 June 2007; published 19 July 2007)

We consider the effect of magnetic impurities, modeled by classical spins, in a conventional superconductor. We study their effect on the quasiparticles, specifically on the spin density and local density of states. As previously emphasized, the impurities induce multiple scatterings of the quasiparticle wave functions, leading to complex interference phenomena. Also, the impurities induce quantum phase transitions in the many-body system. Previous authors studied the effect of either a small number of impurities (from 1 to 3) or a finite concentration of impurities, typically in a disordered distribution. In this work, we assume a regular set of spins distributed inside the superconductor in such a way that the spins are oriented, forming different types of domain walls, assumed stable. This situation may be particularly interesting in the context of spin transfer due to polarized currents traversing the material.

DOI: [10.1103/PhysRevB.76.014512](https://doi.org/10.1103/PhysRevB.76.014512)

PACS number(s): 74.81.-g, 75.60.Ch, 74.25.Ha

## I. INTRODUCTION

The effect of perturbing the superconducting state is a topic of interest since it often provides information about the superconducting state, its nature, and origin. It also provides information about its parent normal state. This has gained particular interest due to the elusive nature of pairing in high-temperature superconductors. In particular, the effect of magnetic fields in its various forms has attracted interest for a long time, such as the effect of vortices in type-II superconductors and, in general, the interplay between superconductivity and magnetic field.

Also, the effect of impurities has been studied considering both nonmagnetic and magnetic impurities in conventional and unconventional superconductors.<sup>1</sup> In the case of nonmagnetic impurities and *s*-wave pairing, Anderson's theorem states that, at least for low concentrations, they have little effect since the impurities are not pair breaking.<sup>2</sup> In *d*-wave superconductors, however, nonmagnetic impurities cause a strong pair breaking effect.<sup>3</sup> In the limit of strong scattering, it was found that the lowest energy quasiparticles become localized below the mobility gap, even in a regime where the single-electron wave functions are still extended.<sup>4</sup> This result has been confirmed solving the Bogoliubov–de Gennes equations with a finite concentration of nonmagnetic impurities.<sup>5</sup> However, allowing for angular dependent impurity scattering potentials, it has been found that the scattering processes close to the gap nodes may give rise to extended gapless regions.<sup>6</sup>

Several conflicting predictions have appeared in the literature regarding the effect of the presence of impurities. Some progress toward understanding the disparity of theoretical results has been achieved realizing that the details of the type of disorder significantly affect the density of states.<sup>7</sup> Particularly in the case of *d*-wave superconductors, in contrast to conventional gapped *s*-wave superconductors, the presence of gapless nodes is expected to affect the transport properties. Using a field theoretic description and linearizing the spec-

trum around the four Dirac-like nodes, it has been suggested that the system is critical. It was obtained that the density of states is of the type  $\rho(\epsilon) \sim |\epsilon|^\alpha$ , where  $\alpha$  is a nonuniversal exponent dependent on the disorder, and that the low energy modes are extended states (critical metal).<sup>8</sup> Taking into account the effects of internodal scattering (hard scattering), it has been shown that an insulating state is obtained instead, where the density of states still vanishes at low energy but with an exponent  $\alpha=1$  independent of disorder.<sup>9</sup> Using the Bogoliubov–de Gennes (BdG) equations, it was found that the *d*-wave superconductivity is mainly destroyed locally near a strong scatterer. The superfluid density is strongly suppressed near the impurities but only mildly affected elsewhere.<sup>10</sup> No evidence for localization of the low energy states was found. The superfluid density is suppressed but less than expected<sup>5,11</sup> and, accordingly, the decrease of the critical temperature with disorder is much slower than previously expected, in accordance with experiments.<sup>12</sup> Similar results of an inhomogeneous order parameter were also obtained for *s*-wave superconductors.<sup>13</sup> The results show that the order parameter is only significantly affected close to the impurity locations.

On the other hand, magnetic impurities induce in-gap bound states in conventional superconductors, while, for instance, in *d*-wave superconductors, due to their gapless nature, they just induce virtual bound states. The local nature of these bound states can now be studied in detail due to the progress in experimental techniques such as scanning tunneling microscopy. In their pioneer work,<sup>14</sup> Abrikosov and Gor'kov considered the properties of a superconductor with magnetic impurities. They demonstrated that the noninteracting magnetic impurities suppress the superconductivity, so that at some critical impurity density the superconducting gap  $\Delta$  shrinks to zero, which was later identified as a quantum critical point.<sup>15</sup>

It was also shown long ago that the presence of few magnetic impurities (vanishing concentration) is enough to lead to rather interesting quantum phase transitions (QPT's), in

particular in the total magnetic moment of the condensate.<sup>16</sup> In the simplest case, the magnetic impurities can be treated as classical spins inserted in the superconductor, acting as local magnetic fields. Indeed, it was shown that if the coupling is weak enough, the Kondo coupling can be overlooked and a much simpler treatment of the classical case provides a good description.<sup>17</sup> Actually, even though there are similarities between the interaction of the electrons with an impurity both in the standard Kondo effect in metals and the coupling to the magnetic impurity in the superconductor, while the Kondo effect is merely a crossover between a free spin at high energies or temperatures and the Kondo singlet (for an  $S=1/2$  impurity in a single  $s$  band) at low energies,<sup>18</sup> in the case of the superconductor there is a true first order quantum phase transition.<sup>19</sup> The phase transition occurs through a level crossing between two states as the coupling between the spin density of the electrons and the impurity spin grows. The level crossing occurs between one state that describes an uncompensated local spin (at smaller coupling) and a state where the impurity spin is compensated (partially since for the classical description to be valid the spin has to be large).

The case of two (or three) impurities has also been studied<sup>20,21</sup> and quantum phase transitions have been identified both as a function of coupling and also as a function of other parameters such as the distance between the impurities and the angle between their spin orientations. Varying judiciously these parameters, one may cross various phase transition points. The richness of these alternations was explained in terms of interference effects between the locally induced states at the impurity sites, in a related way to the study of mirages and other interference effects in other systems.<sup>21–25</sup>

In the case of interacting magnetic moments in a superconductor, the nature of the superconducting transition changes and the critical temperature slightly increases.<sup>26</sup> Recently, Galitski and Larkin studied<sup>27</sup> the effect of a spin-glass ordering of magnetic impurities on the superconductivity. They showed that the superconducting properties depend on the state of the magnetic system and found a shift of the superconducting quantum critical point. A related problem is the mechanism of the exchange interaction of magnetic moments in the superconductor. In the case of normal metal, this is the Ruderman-Kittel-Kasuya-Yoshida (RKKY) interaction due to Friedel oscillations of the magnetic density in the electron gas, induced by a single moment. In the case of a superconductor, the RKKY interaction is affected by the gap at the Fermi surface.<sup>28</sup> This effect was revisited in some recent works.<sup>27,29</sup> The main result is that the form of the RKKY interaction in superconductors is mainly preserved but the interaction contains a decaying exponential factor which vanishes when  $\Delta \rightarrow 0$ .

As is well known, in the case of dominating ferromagnetic long-range ordering of the moments, the competition between superconductivity and ferromagnetism leads to the absence of superconductivity. In other words, ferromagnetism suppresses the superconductivity, acting like an external magnetic field. However, it is possible to reach a coexistence of the magnetization in magnetic domains with the superconducting state.<sup>30</sup> On the other hand, the coexistence of superconductivity and antiferromagnetism is much more

favorable, since on average a Cooper pair, if the coherence length is large enough, will feel a zero magnetic field. In general, the two phases compete with each other but in some cases there is a coexistence. Competition between antiferromagnetic and superconducting orders is an important characteristic of heavy-fermion systems,<sup>31</sup> which is also shared by high- $T_c$  materials<sup>32</sup> and low-dimensional systems.<sup>33</sup> Heavy-fermion systems that exhibit both superconductivity and antiferromagnetism exhibit ratios between the Néel temperature  $T_N$  and the superconducting critical temperature  $T_c$  that can vary substantially (of the order of  $T_N/T_c \sim 1-100$ ), with coexistence of both types of order below  $T_c$ . The coexistence of both types of order can be tuned by external parameters such as externally applied pressure and chemical pressure (involving changes in the stoichiometry).<sup>31,34</sup> It has recently been found that UPd<sub>2</sub>Al<sub>3</sub> ( $T_N=14.3$  K and  $T_c=2$  K) and UNi<sub>2</sub>Al<sub>3</sub> ( $T_N=4.5$  K and  $T_c=1.2$  K) show coexistence of superconductivity and local moment antiferromagnetism.<sup>31,35–38</sup> However, in the Ce-based heavy-fermion, magnetism typically competes with superconductivity. It has been found in the context of the Anderson model that, both in the problem of local moment formation in the superconductor<sup>39</sup> and in the context of the Anderson lattice model, in a certain regime, a quantum phase transition is found<sup>40</sup> which is characterized by an abrupt expulsion of magnetic order by  $d$ -wave superconductivity, as an externally applied pressure increases. This transition takes place when the  $d$ -wave superconducting critical temperature  $T_c$  intercepts the magnetic critical temperature  $T_m$  under increasing pressure.

In our theoretical model, the magnetic moments are considered as a certain magnetic structure embedded into a superconductor. There are different ways to realize it practically by using modern nanotechnology. One of them is related to the formation of a magnetic structure on top of the superconducting layer. As another example, it can also be a laterally organized magnetic superlattice or a hybrid ferromagnet/superconductor (F/S) structure.<sup>41–44</sup>

Various types of heterostructures of superconductors and ferromagnets have been considered in the recent literature.<sup>45–47</sup> Also, the influence of magnetic dots (randomly or regularly distributed) coupled to a superconductor has received attention.<sup>48</sup> In the first case, the proximity effect due to the vicinity of the various systems, where both magnetic fluctuations penetrate the superconductor and superconducting fluctuations penetrate the magnetic system,<sup>49</sup> has received particular attention due to potential device applications. The penetration of the magnetic field in the superconductor splits the up and down spin electron bands, due to the Zeeman effect, in addition to the orbital effect through the vector potential. The Cooper pairs have a finite momentum due to the band splitting and the order parameter oscillates in the superconducting phase. If the size of the superconducting region is small enough, these oscillations have noticeable consequences, such as, for instance, oscillations in the critical temperature of the superconducting region in F/S/F structures<sup>45</sup> or varying relative phases of the superconducting wave functions in S/F/S structures if the thickness of the superconducting region is changed. This has been confirmed looking at the Josephson current through the

heterostructure.<sup>45</sup> In particular, the so-called  $\pi$  junctions, where the Josephson current vanishes, have received attention in the literature.<sup>50,51</sup> In the second case of a distribution of magnetic dots in the close vicinity of the superconductor, it has been shown that if the magnetic moments coupled are oriented via an external field, they act as very effective pinning centers for vortices present in the superconductor<sup>52</sup> originating so-called frozen flux superconductors.<sup>53</sup> The insertion of magnetic rods in the superconductor is also interesting.<sup>54–56</sup>

Now, the interest to the superconductivity on a magnetic profile arises on a quite different ground. It was found that electronic properties of magnetic nanostructures can be used in various magnetoelectronic devices, in which the magnetic state can be effectively controlled by the magnetic field or electric current and, in turn, the variation of the magnetic state changes strongly the electronic characteristics of devices (and vice versa).<sup>57,58</sup> More recently, the semiconducting magnetic materials are included into consideration,<sup>59–62</sup> and the superconductors are also used as some elements of the hybrid structures for magnetoelectronic applications.<sup>63</sup> It seems therefore worthwhile to consider the same type of phenomena in a superconductor with magnetic impurities disposed in some form of ordering that may be controllable from the outside.<sup>64–66</sup> In particular, we have in mind finite systems to which we may attach leads through which we may insert currents that go through a superconducting material with classical spins immersed with their spins oriented in such a way that they form domain walls. These may be achieved, for instance, by imposing different boundary conditions between two sides of the material. Therefore, in this work, we have in mind systems that are finite and with non-periodic boundary conditions.

While it is interesting to consider the effect the superconducting state may have on the magnetic profile in view of possible spintronics applications, it is also interesting to see the effect of the patterned magnetization profile on the superconducting properties. In this work, we focus on the latter aspect of the problem imposing a fixed magnetic pattern. Usually, people consider, say, a semiconductor in a potential quantum well or a metal in a magnetic profile but not a superconductor in a magnetic profile. We find that the impurities affect the properties in a very local way and the pattern of interferences between the impurity induced states is rather complex. We also find quantum phase transitions in these situations. Even though we present our results for a fixed magnetic profile, we also study the stability of the magnetic profile, taking as the stabilizing factor a possible RKKY interaction between the impurities mediated by the quasiparticles of the superconductor.

In Sec. II, we introduce the model that describes the magnetic impurities inserted in the BCS  $s$ -wave superconductor. In Sec. III, we consider the quantum phase transitions originated by the change of the coupling between the classical impurity spins and the conduction electron spin density revealed in the structure of the energy levels, local spin density, local gap function, and global spin density. In Sec. IV, we study the nature of the quasiparticle states revealed in the local density of states and the local kinetic energy. In Sec. V, we consider the stability of the domain wall, taking into ac-

count an effective interaction between the impurity spins that may originate in a RKKY interaction, and in Sec. VI we study the effect of a finite temperature, particularly on the quantum phase transition. We conclude in Sec. VII.

## II. MODEL

Consider a set of classical spins immersed in a two-dimensional  $s$ -wave conventional superconductor. We consider a two-dimensional system for computational simplicity and because it is easier to experimentally control either the location of the magnetic impurities or the local magnetic fields induced by the vicinity of, for instance, magnetic dots. We use a lattice description of the system. In some sites, we place classical spins parametrized like

$$\frac{\vec{S}_l}{S} = \cos \varphi_l \vec{e}_x + \sin \varphi_l \vec{e}_z, \quad (1)$$

where  $S$  is the modulus of the spin. Thus, we assume that the spins lie in the  $x$ - $z$  plane. The Hamiltonian of the system is given by

$$H = - \sum_{\langle i,j \rangle, \sigma} t_{ij} c_{i\sigma}^\dagger c_{j\sigma} - \mu \sum_{i\sigma} c_{i\sigma}^\dagger c_{i\sigma} + \sum_i (\Delta_i c_{i\uparrow}^\dagger c_{i\downarrow}^\dagger + \Delta_i^* c_{i\downarrow} c_{i\uparrow}) - \sum_{i,l,\sigma,\sigma'} J_{i,l} (\cos \varphi_l c_{i\sigma}^\dagger \sigma_{\sigma,\sigma'}^x c_{i\sigma'} + \sin \varphi_l c_{i\sigma}^\dagger \sigma_{\sigma,\sigma'}^z c_{i\sigma'}), \quad (2)$$

where the first term describes the hopping of electrons between different sites on the lattice, the second term includes the chemical potential  $\mu$ , the third one corresponds to the superconducting  $s$  pairing with the site-dependent order parameter  $\Delta_i$ , and the last term is the exchange interaction of an electron at site  $i$  with the magnetic impurity located at site  $l$ . The hopping matrix is given by  $t_{i,j} = t \delta_{j,i+\delta} + t' \delta_{j,i+\delta'}$ , where  $\delta$  is a vector to a nearest-neighbor site and  $\delta'$  to a next-nearest site. Most of our calculations will be performed taking  $t=1$ ,  $t'=0$ , and  $\mu=-1$ . For this value of the chemical potential, the band is between quarter and half-filling. The effects of introducing a next-nearest-neighbor hopping or varying the chemical potential are discussed below. Note that both the indices  $l$  and  $i, j$  specify sites on a two-dimensional system. The indices  $i, j=1, \dots, N$ , where  $N$  is the number of lattice sites. We take  $J_{i,l} = J \delta_{i,l}$  and therefore the last sum is over the sites,  $l$ , where a spin is located. We assume that the spin configuration is fixed and static. Later on, we will study the stability of the spin configuration.

The diagonalization of this Hamiltonian is performed using the Bogoliubov transformation in the form

$$c_{i\uparrow} = \sum_n [u_n(i, \uparrow) \gamma_n - v_n^*(i, \uparrow) \gamma_n^\dagger],$$

$$c_{i\downarrow} = \sum_n [u_n(i, \downarrow) \gamma_n + v_n^*(i, \downarrow) \gamma_n^\dagger]. \quad (3)$$

Here,  $n$  is a complete set of states,  $u_n$  and  $v_n$  are related to the eigenfunctions of Hamiltonian (2), and the new fermionic operators  $\gamma_n$  are the quasiparticle operators. These are chosen such that in terms of new operators,

$$H = E_g + \sum_n \epsilon_n \gamma_n^\dagger \gamma_n, \quad (4)$$

where  $E_g$  is the ground state energy and  $\epsilon_n$  are the excitation energies. As a consequence,

$$\begin{aligned} [H, \gamma_n] &= -\epsilon_n \gamma_n, \\ [H, \gamma_n^\dagger] &= \epsilon_n \gamma_n^\dagger. \end{aligned} \quad (5)$$

The coefficients  $u_n(i, \sigma)$ ,  $v_n(n, \sigma)$  can be obtained by solving the Bogoliubov–de Gennes equations.<sup>67</sup> Defining the vector

$$\psi_n(i) = \begin{pmatrix} u_n(i, \uparrow) \\ v_n(i, \downarrow) \\ u_n(i, \downarrow) \\ v_n(i, \uparrow) \end{pmatrix},$$

the BdG equations can be written as

$$\mathcal{H} \psi_n = \epsilon_n \psi_n, \quad (6)$$

where the matrix  $\mathcal{H}$  at site  $i$  is given by

$$\mathcal{H} = \begin{pmatrix} -h - \mu - J_{i,l} \sin \varphi_l & \Delta_i & -J_{i,l} \cos \varphi_l & 0 \\ \Delta_i^* & h + \mu - J_{i,l} \sin \varphi_l & 0 & -J_{i,l} \cos \varphi_l \\ -J_{i,l} \cos \varphi_l & 0 & -h - \mu + J_{i,l} \sin \varphi_l & \Delta_i \\ 0 & -J_{i,l} \cos \varphi_l & \Delta_i^* & h + \mu + J_{i,l} \sin \varphi_l \end{pmatrix},$$

where  $h = (t\hat{s}_\delta + t'\hat{s}_{\delta'})$  with  $\hat{s}_\delta f(i) = f(i + \delta)$  and  $\hat{s}_{\delta'} f(i) = f(i + \delta')$ . The solution of these equations gives both the energy eigenvalues and eigenstates. The problem involves the diagonalization of a  $(4N) \times (4N)$  matrix. The solution of the BdG equations is performed self-consistently, imposing at each iteration that

$$\Delta_i = \frac{V}{2} (\langle c_{i\uparrow} c_{i\downarrow} \rangle - \langle c_{i\downarrow} c_{i\uparrow} \rangle), \quad (7)$$

where  $V$  is the effective attractive interaction between the electrons. Using the canonical transformation, this can be written as

$$\begin{aligned} \Delta_i = -V \sum_{n, 0 < \epsilon_n < \hbar \omega_D} & \left\{ f_n [u_n(i, \uparrow) v_n^*(i, \downarrow) + u_n(i, \downarrow) v_n^*(i, \uparrow)] \right. \\ & \left. - \frac{1}{2} [u_n(i, \uparrow) v_n^*(i, \downarrow) + u_n(i, \downarrow) v_n^*(i, \uparrow)] \right\}, \end{aligned} \quad (8)$$

where  $\omega_D$  is the Debye frequency, and  $f_n$  is the Fermi function defined as usual like

$$f_n = \frac{1}{e^{\epsilon_n/T} + 1},$$

where  $T$  is the temperature. We note that the Bogoliubov–de Gennes equations are invariant under the substitutions  $\epsilon_n \rightarrow -\epsilon_n$ ,  $u(\uparrow) \rightarrow v(\uparrow)$ ,  $v(\uparrow) \rightarrow u(\uparrow)$ ,  $v(\downarrow) \rightarrow -u(\downarrow)$ ,  $u(\downarrow) \rightarrow -v(\downarrow)$ .

We are interested in calculating various quantities. In particular, we calculate the quasiparticle spin densities,

$$\begin{aligned} s_z(i) &= \frac{1}{2} \langle c_{i,\sigma}^\dagger \sigma_{\sigma,\sigma'}^z c_{i,\sigma'} \rangle \\ &= \frac{1}{2} \sum_n \{ f_n [|u_n(i, \uparrow)|^2 - |u_n(i, \downarrow)|^2] + (1 - f_n) [|v_n(i, \uparrow)|^2 \\ &\quad - |v_n(i, \downarrow)|^2] \}, \\ s_x(i) &= \frac{1}{2} \langle c_{i,\sigma}^\dagger \sigma_{\sigma,\sigma'}^x c_{i,\sigma'} \rangle \\ &= \frac{1}{2} \sum_n \{ f_n [u_n^*(i, \uparrow) u_n(i, \downarrow) + u_n^*(i, \downarrow) u_n(i, \uparrow)] \\ &\quad - (1 - f_n) [v_n^*(i, \uparrow) v_n(i, \downarrow) + v_n^*(i, \downarrow) v_n(i, \uparrow)] \}, \end{aligned} \quad (9)$$

where the sums are taken over the positive excitation energies. Also, we are interested in calculating the local density of states,

$$\rho(\epsilon, i) = \sum_{n,\sigma} [|u_n(i, \sigma)|^2 \delta(\epsilon - \epsilon_n) + |v_n(i, \sigma)|^2 \delta(\epsilon + \epsilon_n)]. \quad (10)$$

Since the system is finite, the states are discrete. This can be written as

$$\rho(\epsilon, i) = \sum_{n,\sigma,\alpha} \rho_\alpha(\epsilon_n, i, \sigma), \quad (11)$$

where  $\alpha = +$  runs over the positive energy eigenvalues of Eq. (6)  $\epsilon_n^+$  and  $\alpha = -$  runs over the negative energies  $\epsilon_n^-$ . Therefore,

$$\rho_\pm(\epsilon_n, i, \sigma) = |u_n(i, \sigma)|^2 \delta_{\epsilon, \epsilon_n^+} + |v_n(i, \sigma)|^2 \delta_{\epsilon, \epsilon_n^-} \quad (12)$$

and

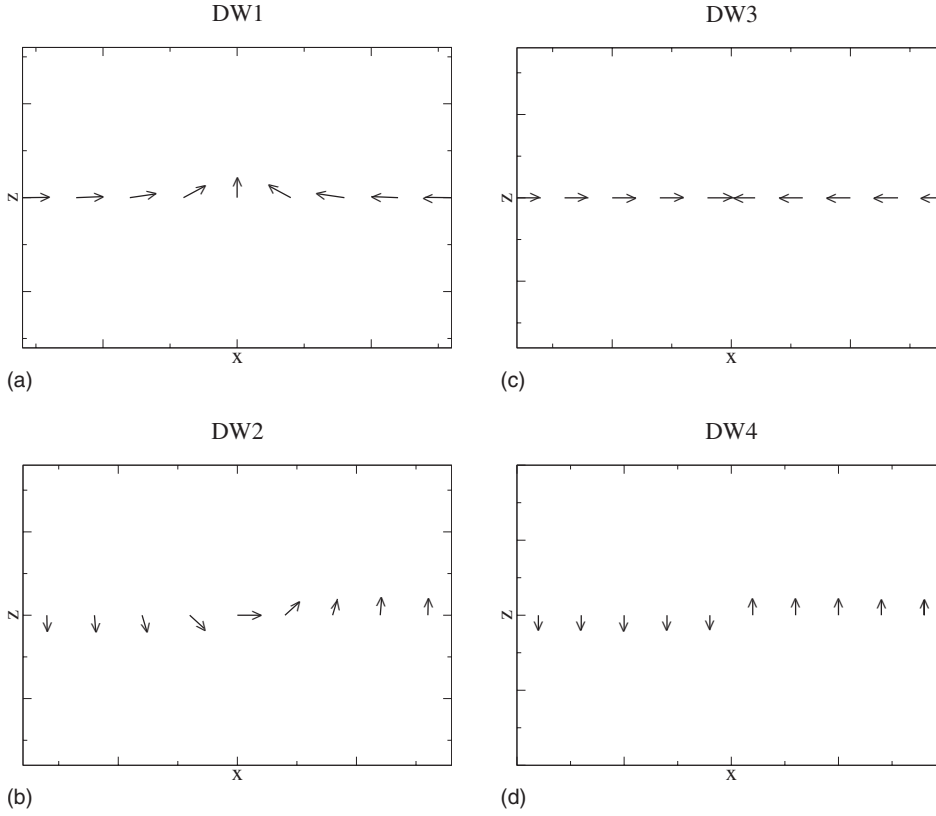


FIG. 1. Various Néel-type domain walls considered in this paper.

$$\rho_-(\epsilon_n, i, \sigma) = |v_n(i, \sigma)|^2 \delta_{\epsilon, \epsilon_n^+} + |u_n(i, \sigma)|^2 \delta_{\epsilon, \epsilon_n^-}, \quad (13)$$

where  $\epsilon_n^\alpha = -\epsilon_n^{-\alpha}$ .

Consider now the possibility that there is a line of impurities,  $\vec{S}_i$ , such that their spin orientations are correlated. For simplicity, we consider a one-dimensional array of spins that traverse the two-dimensional material from one border to the other along the  $x$  direction. A dense impurity distribution will destroy superconductivity if the spin coupling is strong enough. Therefore, to study the effects of interference, we limit ourselves to lines of spins in the two-dimensional electronic system. One may impose a magnetic field at each side of the sample such that it orients the first and last spins. Choosing different boundary conditions, we may create different domain walls assuming that there are interactions between the spins that tend to orient them. These interactions may either be ferromagnetic or antiferromagnetic and may have its origin in RKKY-type interactions via the superconducting substrate. As we mentioned before, the form of the interactions mediated by the quasiparticles has a form similar to the one of a standard metal.

Clearly, if the number of spins increases considerably and/or their coupling to the electron density increases, enough superconductivity will be destroyed. We will be focusing on situations where superconductivity prevails, as evidenced by the self-consistent solution of the BdG equations. In particular, if we consider a fully two-dimensional distribution of classical spins, unless the coupling is small, in general, superconductivity will be destroyed.

The various cases considered are displayed in Fig. 1. Besides the cases of one impurity and two impurities previously

considered, and that we briefly consider here to compare with the new results, we consider various situations where, for instance, we have a domain wall of the Néel type (here limited to a line of spins to simplify) where the leftmost spin is either oriented along the chain (defined as the  $x$  direction) or perpendicularly to it (these are the cases DW1 and DW2, respectively). Specifically, in the case of domain wall DW1, we choose

$$\varphi_l = \frac{\pi}{2} + \frac{\pi}{2} \tanh \frac{x - x_c}{\lambda}, \quad (14)$$

and, for the domain wall DW2,

$$\varphi_l = \frac{\pi}{2} \tanh \frac{x - x_c}{\lambda}. \quad (15)$$

The other configurations are characterized by  $\varphi_l = \frac{\pi}{2} \theta(-x) - \frac{\pi}{2} \theta(x)$ , for the domain wall DW3,  $\varphi_l = \pi \theta(-x)$  and  $\varphi_l = 0$  for  $x > 0$ , for DW4, and  $\varphi_l = \frac{\pi}{2} [1 + (-1)^x]$ , for the antiferromagnetic (AF) case, DW5.

Most of our results were obtained for a system of  $15 \times 15$  sites. Increasing the system size does not affect qualitatively the results. For instance, we have considered a system of  $25 \times 25$  sites and the results are very similar. The only visible difference is the reduction of the finite size effects near the borders of the system. We used parameters such that superconductivity is stable and the superconducting gap is relatively large so that the in-gap states are easily identified. Choosing units where the hopping  $t=1$ , we get a gap of the order of 0.4 choosing  $V=4t$ . Typically, we choose  $\lambda=3$ .

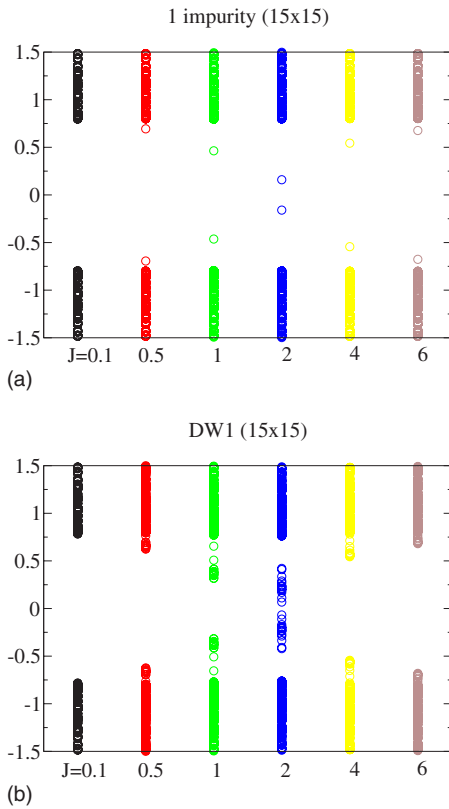


FIG. 2. (Color online) (a) Energy levels for one impurity. There is one pair of bound states originated by the impurity. As  $J$  grows, the level appears to “cross” zero energy. The crossing is between  $J=1$  and  $J=2$  (see below). (b) Energy levels for DW1 domain wall.

### III. QUANTUM PHASE TRANSITIONS

#### A. Energy levels

We begin by revisiting some results for a situation where we have one or two impurities immersed in the material. As is typical of an  $s$ -wave pairing, the clean system has a gap. Introducing one magnetic impurity generates two bound states in the gap. One is at positive energies and the other is at a symmetric negative energy. This is clearly shown in Fig. 2. The nature of the wave functions corresponding to the two eigenstates will be discussed later. If we introduce two impurities, the number of states in the gap doubles. In general, if there are  $N_i$  impurities, there are  $2N_i$  states in the gap,  $N_i$  at positive energies and the same at negative energies. As the coupling between the electron spin density and the impurity spin grows, the energy of the bound state lowers and approaches the Fermi level. Increasing further the coupling, the level is repelled from the chemical potential. The nature of the ground state has changed, as we will see below.

In Fig. 2, we also show the energy spectra for the domain wall DW1 for different values of the coupling. There are now as many bound states as impurity spins (for positive energies). For small coupling, the energy levels are close to the top of the gap, but as the coupling grows the trend is similar to the single impurity case. For a large system, the gap will be virtually filled close to the transition where the level crossing(s) takes place. As we will see, there are several level

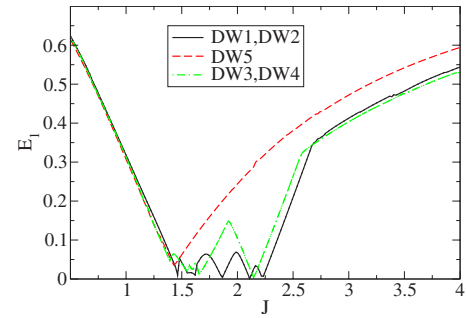


FIG. 3. (Color online) Lowest energy level as a function of  $J$  for the various domain walls. Note the various level crossings (near zeros) for the various cases. The crossings are concentrated for  $1 < J < 2$ . Note that for the antiferromagnetic chain, there is a single level crossing. Domain walls DW1 and DW2 have the same lowest state energy and the same happens with domain walls DW3 and DW4.

crossings as the coupling varies. Note that  $J$  actually means  $JS$ , where  $S$  is the magnitude of the local spins. Therefore, we may consider  $S=1/2$  and change the Zeeman term coupling value. However, we can as well consider that the coupling is not changing much but we are inserting impurity spins with different values of  $S$ . This is truly the classical limit. Previously, the effect of the change in the relative angles or distances between two impurities was considered.<sup>20</sup> These changes also induce changes in the energy spectra and affect the various level crossings. The change in relative angles and/or distances between two impurities in the case of domain walls corresponds to the change in the width of the domain wall,  $\lambda$ . However, the analysis of these interference effects on the states is more complex due to the multiple scatterings, as we will show below.

In contrast to the case of a small number of isolated magnetic moments creating a number of levels in the gap, an ordered array of impurities creates some minibands. It can be clearly seen in Fig. 2, even though we performed our calculations for a finite system.

The detail of the level crossings is better studied considering the evolution of the lowest level (with positive energy) as a function of the coupling  $J$ . This is shown in Fig. 3 for various systems. In the case of a single impurity, there is a single level crossing, which for our parameters occurs at a value between  $J=1$  and  $J=2$ . In the case of the domain walls, there are several level crossings, as illustrated in Fig. 3. For the same set of parameters, the level crossings are contained in an interval of coupling strengths that is of the same order. We recall that at each level crossing, the lowest energy does not strictly reach zero. At a finite value of the coupling, the crossing occurs without closing the gap, indicating that the quantum phase transition is actually a first order one. The same occurs in the cases of the domain walls. However, since the number of bound states inside the gap increases, the minigaps near the various transitions are quite small and in the thermodynamic limit should become vanishingly small. Even for a small system, considering, for instance, a two-dimensional distribution of impurity spins, one expects that the gap will be filled with states. Actually, for a moderate coupling of the order of  $J \sim 1$ , the superconductiv-

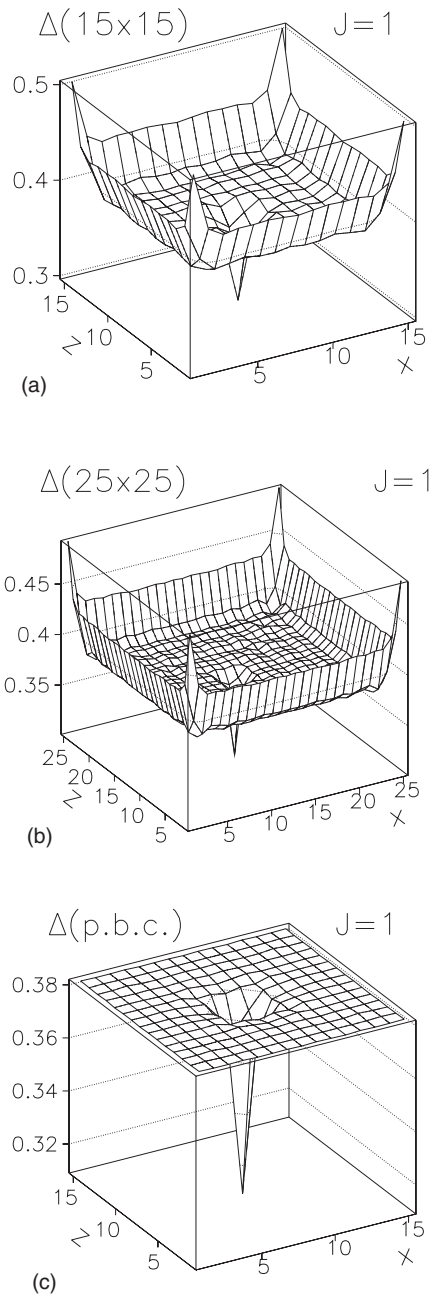


FIG. 4. Comparison of the spatial dependence of the gap function for the case of a single impurity, for the cases (a)  $15 \times 15$  and (b)  $25 \times 25$  for open boundary conditions and (c) periodic boundary conditions, for  $J=1$ .

ity can be destroyed by the local magnetic fields created by the impurities. The states in the gap are localized, as will be shown later.

### B. Local gap function

A characteristic of the order in the system is given by the behavior of the superconducting order parameter, as a function of space.<sup>68</sup> In Fig. 4, we study the effects of system size and boundary conditions on the gap function in the case of a single impurity located at the center of the system. We see

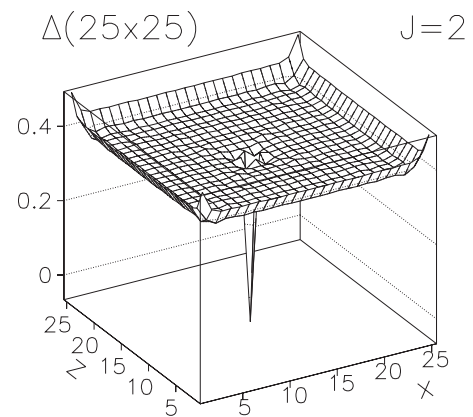


FIG. 5.  $\Delta$  for  $J=2$  for one impurity.  $\Delta$  decreases at the impurity site (this is the same as for a nonmagnetic impurity). Note that there is a  $\pi$  shift in  $\Delta$  (it becomes negative) at the impurity site in contrast to the case for  $J=1$ , shown in Fig. 4(b).

that for open boundary conditions, the finite size effects are important near the border of the system. Increasing the system size, these diminish. In the case of periodic boundary conditions, the finite size effects are virtually absent. Note that away from the borders, the results for the cases  $15 \times 15$  and  $25 \times 25$  are qualitatively the same. Therefore, in the rest of the paper, we will illustrate the results considering either system size preferring, however, the smaller system size since this decreases the computational time. Also, as discussed above, we are aiming at the equilibrium properties of a system which is finite, and therefore we will consider the open boundary conditions instead of the more standard periodic boundary conditions.

In Fig. 5 we consider  $\Delta$  for the typical coupling  $J=2$  for the case of one impurity. The first thing to notice is that the order parameter is only affected very close to the impurity site. Since we are using open boundary conditions, the behavior of the order parameter and other quantities is also affected near the border. If we were to use periodic boundary conditions, these effects would be strongly reduced and for a relatively large system they would be almost vanishing. We note, however, that near the impurity, the boundary conditions have no effect as expected. We note the previously observed  $\pi$  shift of the order parameter when  $J$  is large enough. This effect prevails when we have several impurities. We see from Figs. 6 and 7 that the  $\pi$  shift is observed for the more complex structures, indicating once again that some properties are of a local nature. Also, we see that the orientation of the spins does not affect significantly the order parameter. This is to be expected since we are considering singlet pairing and therefore rotationally invariant. While the spin density is obviously strongly dependent on the impurity spin orientation, the order parameter is only mildly affected particularly at the center of the solitoniclike spin configuration. If the coupling is strong enough, the order parameter is basically constant along the impurity line.

As the level crossings occur, there is a change of phase of  $\pi$  locally, as evidenced by the single impurity results. Therefore, as the various level crossings occur in the cases of several impurities, there may be inhomogeneities since the

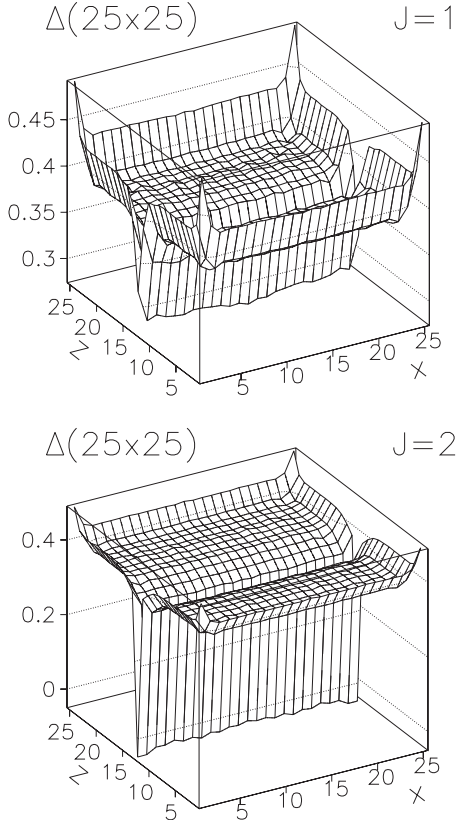


FIG. 6.  $\Delta$  for DW1 for  $J=1,2$ . Note that for  $J=2$ , there is again a  $\pi$  shift.

capture of the electrons by the impurities is not necessarily uniform, as evidenced by the nonhomogeneous changes of local spin density. Therefore, it is natural to expect some inhomogeneities along the chain. This is also seen in the local density of states (LDOS) shown below.

A simple explanation for the occurrence of the  $\pi$  shift is not available.<sup>1</sup> It is argued that it is related to the  $\pi$  junctions referred to above, but these occur for specially commensurate widths of the ferromagnetic slab in  $I/S/F/S$  heterostructures. Here, the effect is quite local and therefore a relation is not clear.

### C. Local spin density

In Figs. 8(a) and 8(b), we show the behavior of the electron spin density in the presence of two impurities. Since the impurity spin acts like a local magnetic field, we expect that the spin density will align along the local field. At the impurity site, the spin density is aligned, as shown in the figure. In Fig. 8, we compare two values of the coupling. For  $J=1$ , note the negative spin density around the impurity site. At the impurity site, it is positive, as expected. For larger  $J$  such as  $J=2$ , notice that the spin density in the vicinity of the impurity site is now positive. We will see that for  $J=1$ , the total  $s_z=0$ , while for larger values of  $J$  it is positive (this is one of the hallmarks of the phase transition). One interpretation is that if  $J$  is strong enough, the impurity captures one electron breaking a Cooper pair leaving the other electron

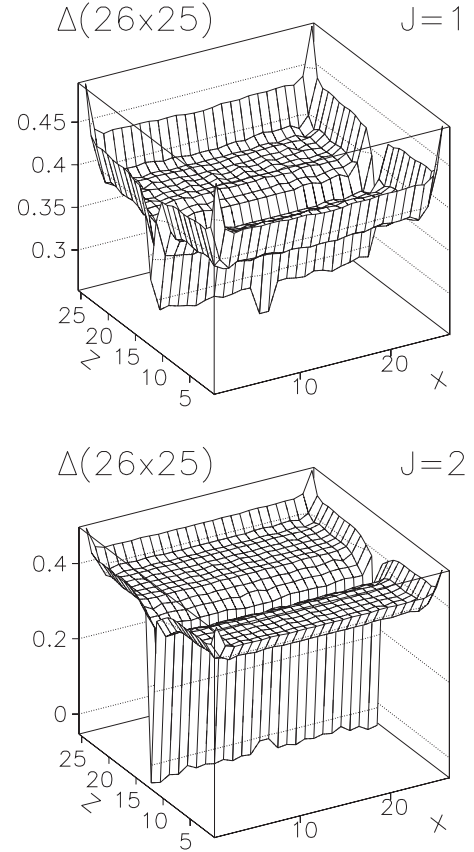


FIG. 7.  $\Delta$  for DW4 for  $J=1,2$ . Once again there is a  $\pi$  shift.

unpaired and the overall electronic system becomes polarized. At zero temperature, where the quantum phase transition occurs, the magnetization reduces to

$$s_z(i) = \frac{1}{2} \sum_{n, \epsilon_n > 0} [|v_n(i, \uparrow)|^2 - |v_n(i, \downarrow)|^2] \\ = \frac{1}{2} \sum_{n, \epsilon_n < 0} [|u_n(i, \uparrow)|^2 - |u_n(i, \downarrow)|^2], \quad (16)$$

and therefore may be calculated either from the hole states at positive energies (given by  $v_n$ ) or by the particle states at negative energies (given by  $u_n$ ). At zero temperature, there are no quasiparticles and therefore all the states of positive energies are empty. We will see later the nature of the states as a function of coupling and their relation to the spin orientation.

In Figs. 8(c)–8(f), we show the results for the spin density for two typical cases, DW1 and DW4, for the same couplings. For  $J=1$ , the first level crossing has not yet occurred and the total magnetization is zero, as for the single impurity case. This implies that the system responds to the local polarization of the electronic spin density at the impurity site by an overall negative polarization, to yield a total magnetization that vanishes. Since the effect of the impurities is quite local, it is around the impurity line that the magnetization is negative. This happens for both domain walls. Increasing the coupling, for instance,  $J=2$ , the situation



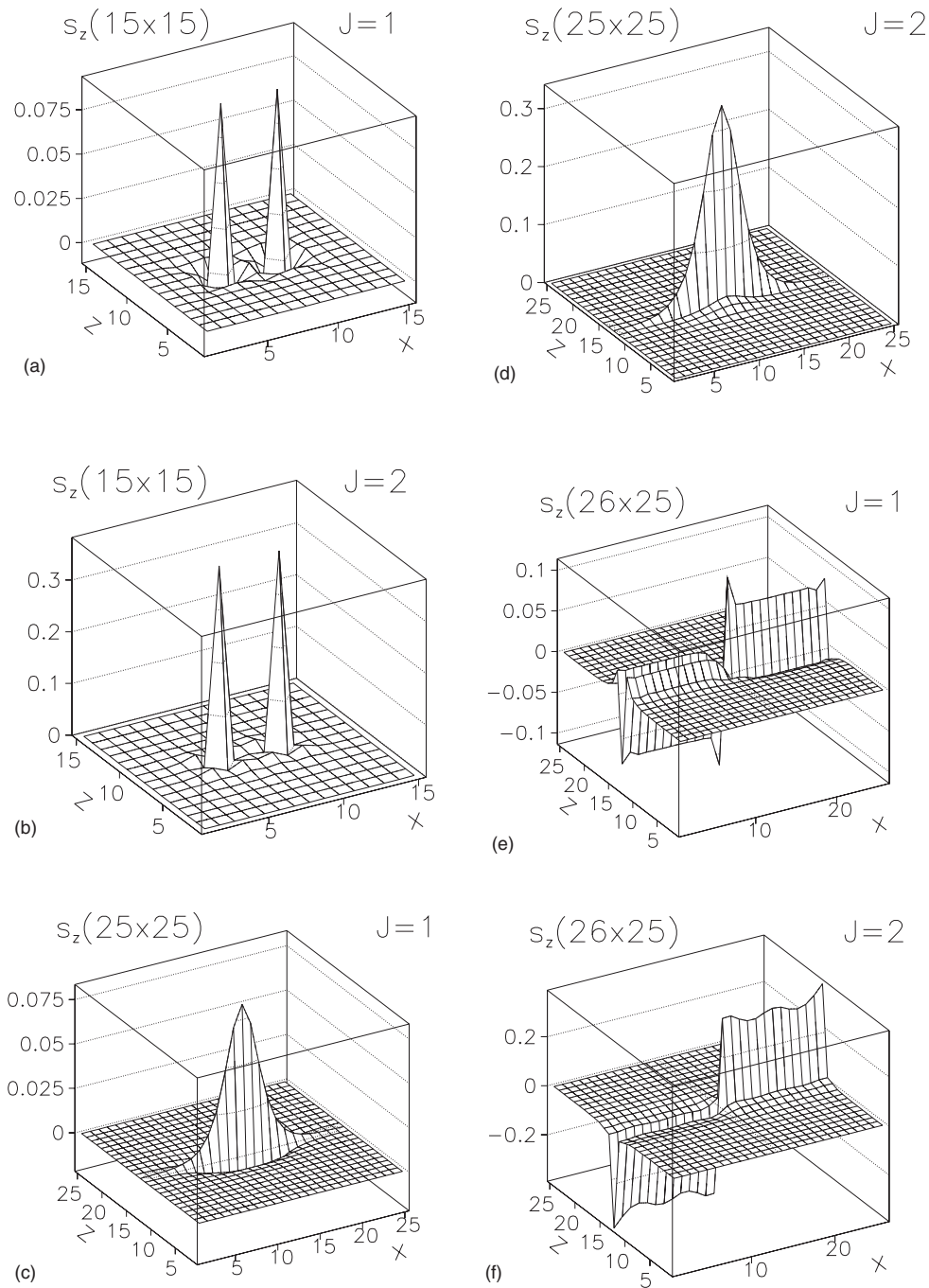


FIG. 8. [(a) and (b)] Plots of  $s_z$ , the local  $z$  component of the electronic spin density for the case of two impurities for  $J=1, 2$ . [(c) and (d)] Plot of  $s_z$  for  $J=1, 2$  for DW1. Note that along the line of spins constituting the domain wall, the spin density is large and positive and that for  $J=1$  in the neighbors it is negative, and for the other case  $J=2$  it is positive. As for the cases of one and two impurities, this transition is associated with a transition from  $s_z^T=0$  to an  $s_z^T \neq 0$ . [(e) and (f)] Plot of  $s_z$  for  $J=1, 2$  for DW4. Note that now the total magnetizations are zero but if we divide the system in two-halves, similar considerations apply.

changes. It is clear from the figures that around the impurity line, the magnetization is no longer negative. The influence of the impurity spins is now strong enough to polarize the electronic system, not only at the impurity sites but also in their vicinity. The total magnetization no longer vanishes but has a finite value. This is further discussed below.

As the coupling changes, in general, the magnetization varies in a continuous way. However, as the system goes

through the various phase transitions, the spin density changes discontinuously consistently with a first order quantum phase transition. Since there are now several spins that may bind electrons in succession, there is now a sequence of phase transitions. These changes are not, in general, uniform along the line of impurities. For instance, in the case of the domain wall DW1 at the first transition (which, for the parameters chosen, occurs near  $J=1.55$ ), there is an increase

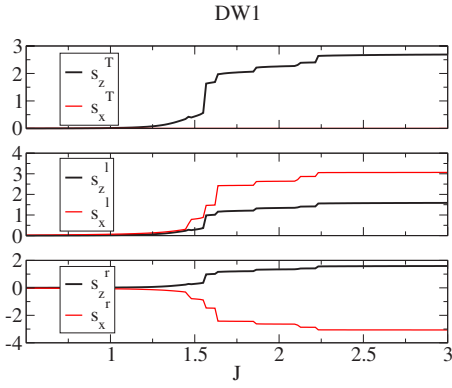


FIG. 9. (Color online) Various quantities for DW1 as a function of  $J$ . We plot  $s_z^T, s_x^T, s_z^l, s_x^l, s_z^r, s_x^r$ . Here,  $l$  and  $r$  stand for left half of the system and right half of the system. Due to the symmetry of the domain wall chosen,  $s_x^T=0$ . Note, however, that if we consider the magnetization of the left or right halves, there are interesting phase transitions.

centered around the middle point of the chain; for the next transition (around  $J=1.62$ ), the increase occurs both at the middle point and at both ends of the chain; and at the next transition (around  $J=1.8475$ ), there is a sharp peak at the middle point and at the transition around  $J=2.215$  the increase has a broad maximum centered around the middle point. This inhomogeneity is characteristic of the various domain walls, where the space distribution of the wave functions is complex due to the multiple interferences of the quasiparticles off the various impurities.

**D. Global spin density**

The sequence of the quantum phase transitions is also clearly displayed if we consider the total magnetization of the system as a function of the coupling. In the cases of the domain walls DW1 and DW2, the total value of  $s_z^T$  and  $s_x^T$  changes as a function of the coupling in basically the same way since one may obtain one case from the other by a rotation in spin space. However, the other domain walls considered have no overall magnetization in any direction. We may, however, consider only the left or right magnetizations

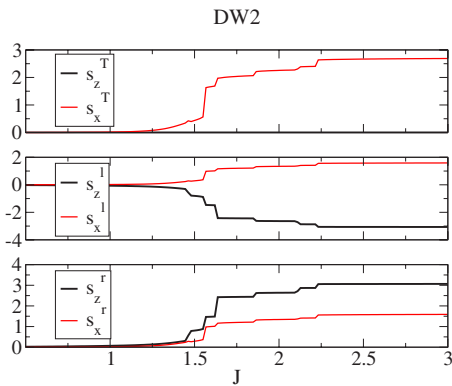


FIG. 10. (Color online) Various quantities for DW2 as a function of  $J$ . We plot  $s_z^T, s_x^T, s_z^l, s_x^l, s_z^r, s_x^r$ .

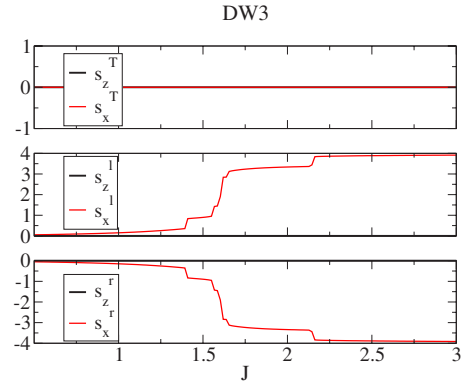


FIG. 11. (Color online) Various quantities for DW3 as a function of  $J$ . We plot  $s_z^T, s_x^T, s_z^l, s_x^l, s_z^r, s_x^r$ .

and these will display the same type of quantum phase transitions, even though the total magnetizations are in principle zero.

The detail of the dependence on the coupling value is better shown in Figs. 9–13 where we present various average spin densities for the various domain walls. Due to the shape of the domain walls, in some cases the total spin densities, summed over all electron sites, vanish. However, the quantum phase transitions are clearly shown if we take averages over, say, half of the system. Associated with the various level crossings, there are various phase transitions between plateaus corresponding to an increasing spin density component as the electron spins bind to the impurity spins.

The antiferromagnetic case is peculiar. There are no true discontinuities but the left and right  $s_x$  do not vanish and show an interesting change of sign at a value of  $J \sim 1.4$ . This is probably a finite size effect that should disappear as the system size increases.

**E. Effect of changing the Fermi level and effect of next-nearest-neighbor hopping**

We have chosen to work with a chemical potential of  $\mu = -1$ . The electron density is therefore not fixed and has to be determined self-consistently. We do not present here the results for the electron density but will consider them in future publications, particularly in the context of transport proper-

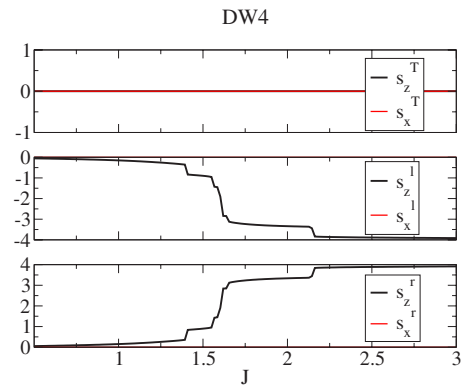


FIG. 12. (Color online) Various quantities for DW4 as a function of  $J$ . We plot  $s_z^T, s_x^T, s_z^l, s_x^l, s_z^r, s_x^r$ .

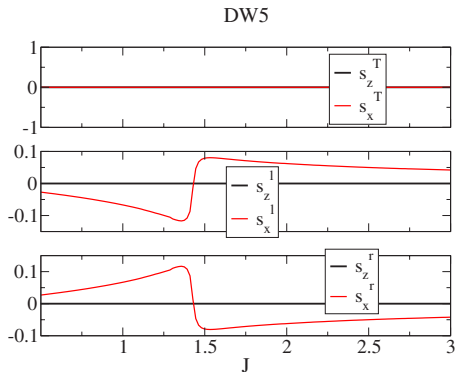


FIG. 13. (Color online) Various quantities for the AF spin configuration (DW5) as a function of  $J$ . We plot  $s_z^T$ ,  $s_x^T$ ,  $s_z^l$ ,  $s_x^l$ ,  $s_z^r$ , and  $s_x^r$ .

ties where the density of charge carriers will play an important role. The results do not depend in a significant way on the value of the chemical potential. The value of  $\mu=-2$  has been chosen before since the system in this case is quarter filled and the analysis of the interference pattern for the two impurities case is simplified,<sup>21</sup> since along the  $x$  axis the Fermi momentum is  $\pi/2$ . In the case of this paper,  $\mu=-1$  means that the band filling is larger but is of the order of 0.65 and therefore is still quite far from half-filling. The change in the chemical potential slightly affects the location of the

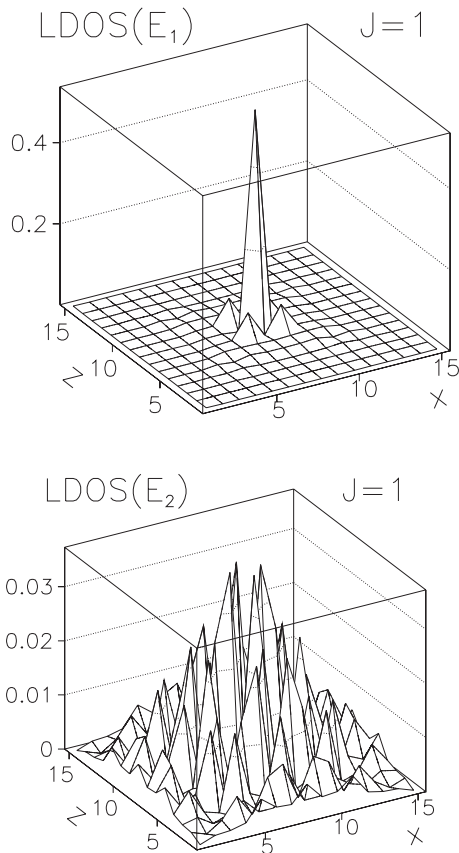


FIG. 14. LDOS for the lowest energy state (with positive energy) and the second lowest state (also with positive energy) for  $J=1$  in the case of a single impurity.

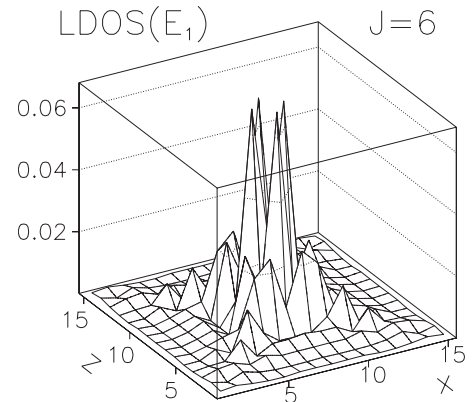
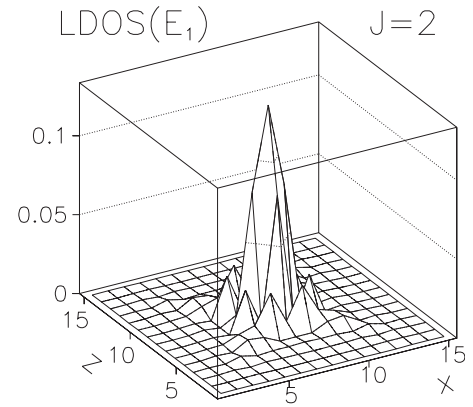


FIG. 15. LDOS for the lowest energy state (with positive energy) for  $J=2,6$  in the case of a single impurity.

quantum phase transitions but the results are qualitatively the same. However, changing the chemical potential affects the band filling. The band filling is also affected by the spin coupling. As the coupling grows, the band filling increases since electrons are trapped by the impurities. We note that if we consider a more realistic situation, where we take into account next-nearest-neighbor hopping, the results are also qualitatively the same. The effect of this extra term is to change the location of the quantum phase transition points. Both decreasing the band filling and introducing the next-nearest-neighbor hopping decrease the order parameter and therefore increase in proportion the importance of the coupling between the spin density and the impurity spin anticipating the appearance of the quantum phase transition.

We note that considering the case of a more dense impurity spin distribution will both tend to destroy superconductivity for smaller values of the coupling and also to increase the band filling approaching the half-filling situation for moderate values of the coupling. This effect will be considered elsewhere.

#### IV. NATURE OF STATES

##### A. Local density of states: $\rho(\epsilon, i)$

As mentioned before, since the spectrum is discrete and symmetric, the density of states is composed by a series of

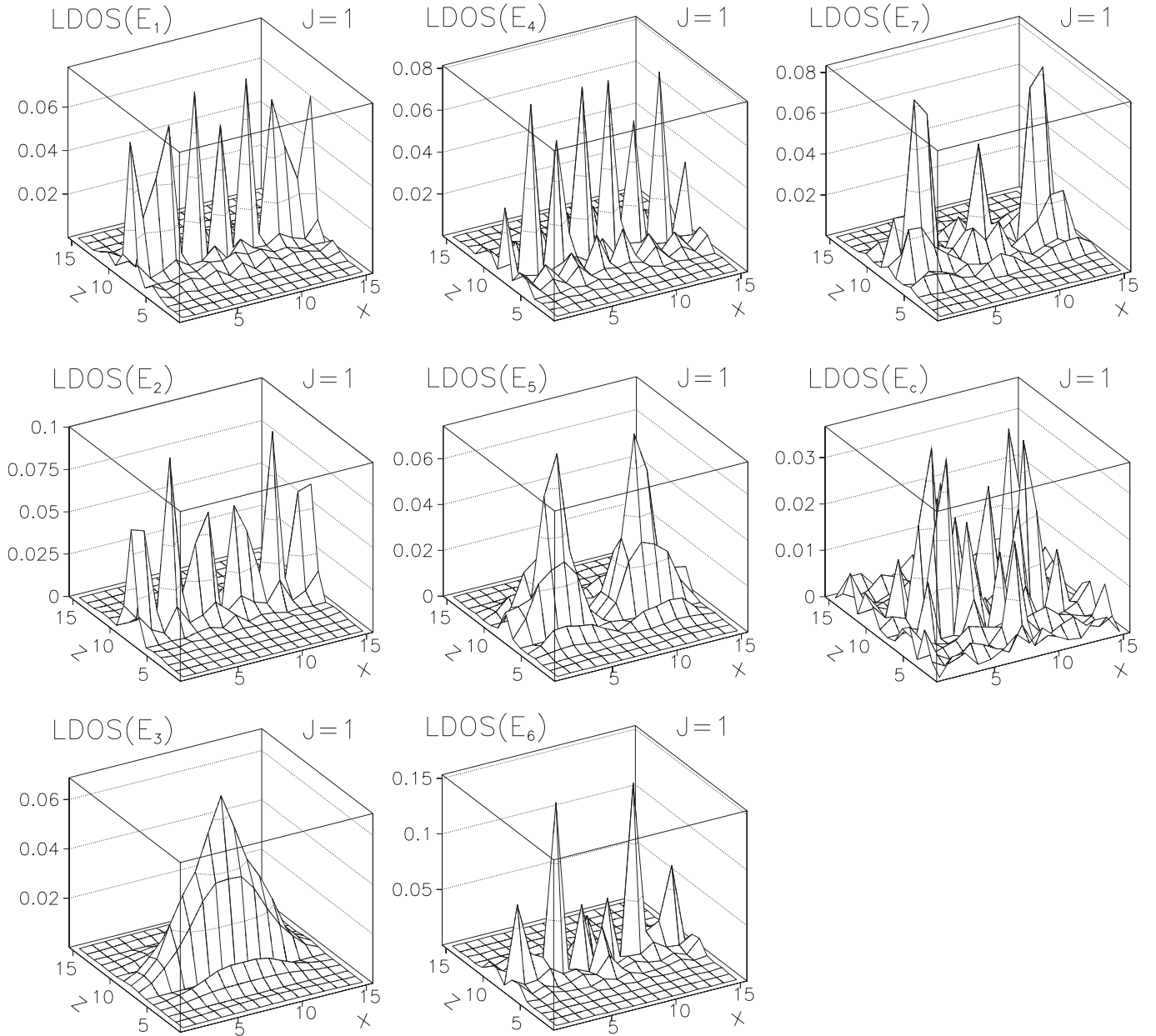


FIG. 16. LDOS for DW1 for the first seven levels for  $J=1$  and a state in the continuum.

delta function peaks, where for each energy (for instance, positive) there are two contributions, one from a level of positive energy, for instance  $\epsilon_n$ , with weight  $|u_n(i, \sigma)|^2$  and another from the symmetric energy level with energy  $-\epsilon_n$  with weight  $|v_{\bar{n}}(i, \sigma)|^2$ , where  $\bar{n}$  is the level symmetric to the level  $n$ .

Consider first the case of a single impurity. The true nature of the bound state of positive energy is better evidenced by the LDOS at the energy of the lowest level. Specifically, and calling this energy level  $n=1$ , the LDOS is given by

$$\begin{aligned} \rho(\epsilon = \epsilon_1, i) &= \sum_{\sigma} [|u_1(i, \sigma)|^2 + |v_{\bar{1}}(i, \sigma)|^2] \\ &= \rho_+(\epsilon_1, i, \uparrow) + \rho_+(\epsilon_1, i, \downarrow). \end{aligned} \quad (17)$$

This is shown in Fig. 14, where the LDOS of the second level (located in the continuum) is also shown for comparison. The LDOS of the second level is spread over the system. The lowest state is localized near the impurity site. The LDOS of the lowest peak is nicely confined around the impurity site and has a large spectral weight. Here, we considered  $J=1$ . Notice that the oscillations are strongly damped beyond the nearest neighbors. In Fig. 15, we consider higher values of the coupling  $J=2, 6$ . Notice that for  $J=2$ , the peak has broadened but is still quite localized. Also, the oscillations are now less damped particularly along the diagonals of the square. Note also that the spectral weight at the impurity site is now reduced. In the case of a large coupling  $J=6$ , the peak is still localized but has several new features. It has a broader spectral weight and there is no peak at the central

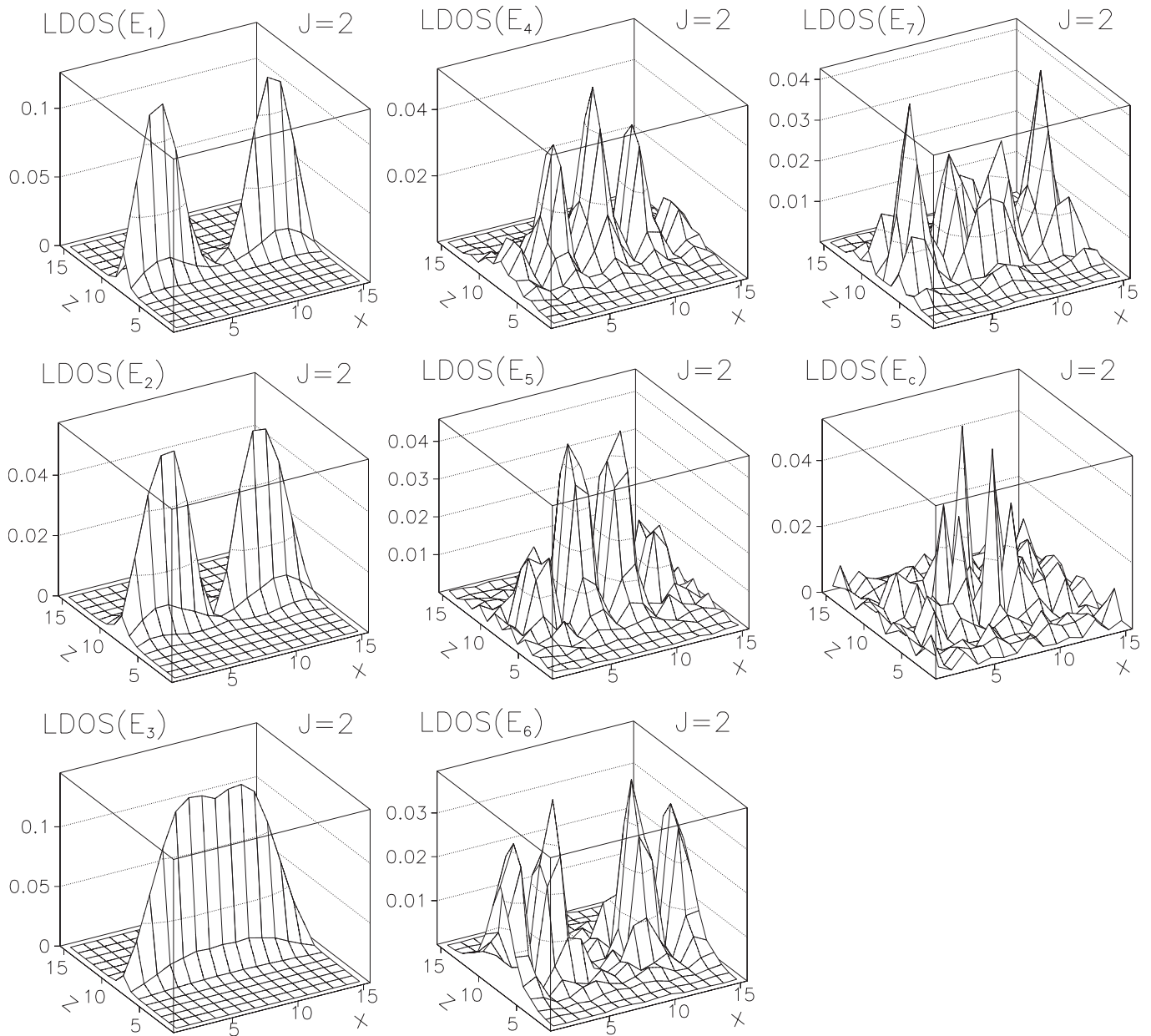


FIG. 17. LDOS for DW1 for the first seven levels for  $J=2$  and a state in the continuum.

point. At the impurity site, the gap function is still negative even though its magnitude decreases for this large  $J$  value. Instead of a central peak, there are now four peaks in the nearest neighbors of the impurity site and a square symmetry, even though the state is still quite localized. Note the extension of the wave functions along the diagonals of the system.

If we consider the case of two impurities, there are now two bound states. The behavior is quite similar to the case of a single impurity with two maxima localized in the vicinity of the impurity sites. The third level and beyond are extended, as expected.

In the cases of a few impurities, like two or three impurities, a study of the relation between the phase transitions and the level structure is possible.<sup>21</sup> However, increasing the number of impurity spins, this analysis is complicated by the multiple interferences of the wave functions of the bound

states. We may, however, look at the LDOS for the lowest levels and examine their structure. This is shown in Figs. 16 and 17 for the domain wall DW3 for the couplings  $J=1, 2$ .

The case of  $J=1$  is similar to the case of a small coupling, where no phase transition has occurred, and the local magnetic field is a small perturbation. Clearly, as the coupling increases, the shielding of the perturbation in the vicinity of the impurity site increases but no qualitative change is observed until the first level crossing. There are now as many bound states as impurities and therefore there are several “localized” states. In Fig. 16, we show the LDOS for the first seven positive energy levels and for a level in the continuum. The states in the gap have a structure along the line of impurities and, in that sense, they are localized. However, since there are several impurities, there is a series of maxima and minima at the impurity sites. In the single impurity or two

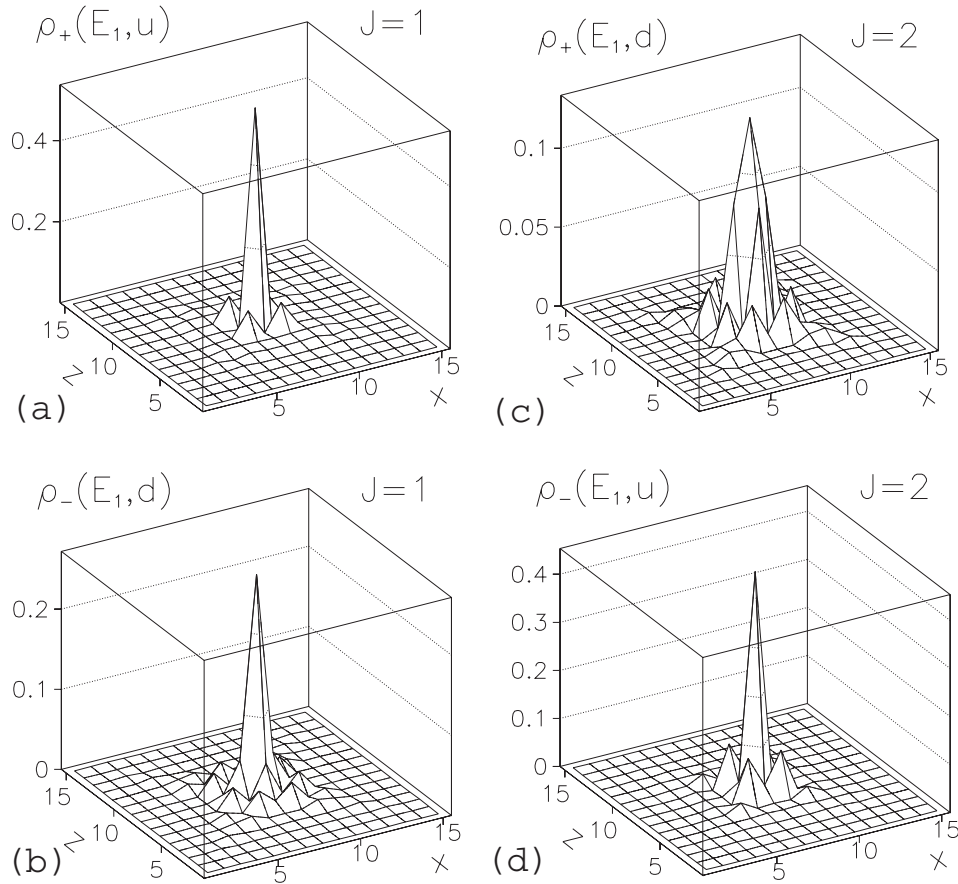


FIG. 18. LDOS for a single impurity. (a)  $\rho_+(\epsilon_1, i, \uparrow)$  for  $J=1$ , (b)  $\rho_-(\epsilon_1, i, \downarrow)$  for  $J=1$ , (c)  $\rho_+(\epsilon_1, i, \downarrow)$  for  $J=2$ , and (d)  $\rho_-(\epsilon_1, i, \uparrow)$  for  $J=2$ . (Note that in the vertical axis, labels  $u=\uparrow$  and  $d=\downarrow$ .)

impurity cases, the bound states have maxima at the impurity locations but we see from Fig. 16 that this is not so. For instance, the lowest level wave function has a series of peaks at alternating sites symmetrically around the central point (note that the number of sites is odd). On the other hand, the second level has a zero at the central point indicative of an antisymmetric state. This is reminiscent of the results obtained for two impurities<sup>21</sup> where there are naturally two states, one symmetric and one antisymmetric. On the other hand, the third peak is quite spread along the domain wall and extends further along the perpendicular direction. As the energy increases, the states are still fairly localized with more or less complex structures. As before, the state in the continuum is of a different nature and spread through the system, even though not homogeneously. The spectral weights are similar even though their magnitudes are correlated inversely with their extension, as expected.

Increasing the coupling to  $J=2$  changes somewhat the wave functions. The first levels are still localized but with different spatial distributions. For instance, the two lowest levels display two broad peaks and deep minima at the central position of the domain wall. The third level is somewhat similar to the case of  $J=1$ . Also, we see an alternancy of symmetric and antisymmetric states as the energy increases.

We should note that the results obtained for the  $15 \times 15$  system are not general. For instance, considering the case of

a  $25 \times 25$  system, the details of the LDOS are different. In particular, due to the increased number of bound states, the sequence of states is more complex. Also, the increased number of states in the gap increases the near degeneracies of the states and mixes their symmetry properties. As discussed above, as the spin coupling grows, the impurities capture electrons. In the case of the extended spin configurations, since the states are extended along the chain of spins, even though the lowest states are localized in the perpendicular direction, it is not possible to disentangle the capture of the electrons by each impurity since the states are a superposition over many sites.

### B. Local density of states: $\rho_\alpha(\epsilon, i, \sigma)$

It is perhaps clearer if we look into greater detail into the LDOS, separating the spin components and trying to understand better the difference between the positive and the negative energy states. Consider once again the case of a single impurity. Let us focus our attention on the first two levels, the first localized and the next in the continuum. Actually, these constitute a set of four states due to the positive and negative energies. The analysis of the LDOS shows that for  $J=1$ , considering first the positive energies, the first level has only a contribution from spin  $\uparrow$  and the first level with negative energy (symmetric to the other level) has only contribu-

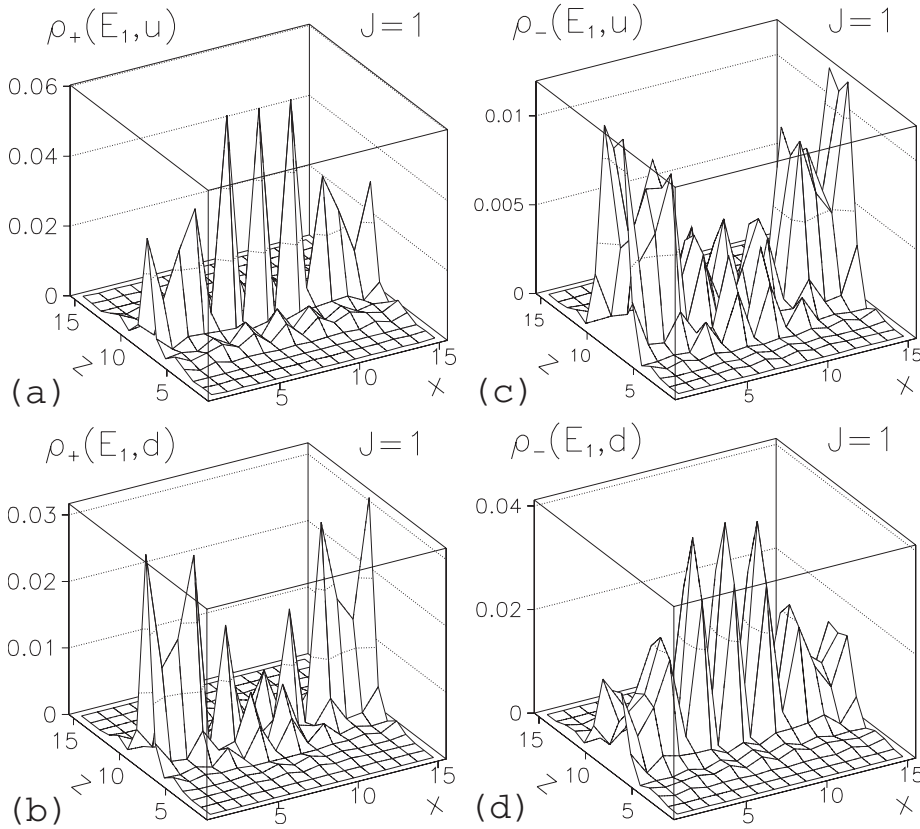


FIG. 19. LDOS for the domain wall DW1. (a)  $\rho_+(\epsilon_1, i, \uparrow)$  for  $J=1$ , (b)  $\rho_+(\epsilon_1, i, \downarrow)$  for  $J=1$ , (c)  $\rho_-(\epsilon_1, i, \uparrow)$  for  $J=1$ , and (d)  $\rho_-(\epsilon_1, i, \downarrow)$  for  $J=1$ . (Note that in the vertical axis, label  $u=\uparrow$  and  $u=\downarrow$ .)

tion from spin  $\downarrow$ . The magnitude of the spectral weight at the impurity site is different for the two states, as already noticed before.<sup>21</sup> In Fig. 18, we show the results for the bound states for both  $J=1$  and  $J=2$ . Considering now the second level located in the continuum, both at positive and negative energies, we obtain that there is a mixture of both spin components, even though in the case of the state at positive energy the magnitude of the peak is larger for the case of spin  $\uparrow$  than for the case of spin  $\downarrow$  and in the case of the state in the continuum at negative energy the relative magnitudes of the two spin components are reversed. Considering now the case of  $J=2$ , where the level crossing has occurred, the nature of the states changes. The positive energy bound state has now only a contribution from the spin  $\downarrow$  component and vice versa, and the first negative energy state has only contribution from the spin  $\uparrow$  component. As the level crossing occurred, the spin content has changed. In Fig. 18, we only show the nonvanishing contributions. The other contributions vanish. On the other hand, in the first state in the continuum, where the two spin components contribute, the magnitude of the  $\uparrow$  component is now much larger than the  $\downarrow$  component, while in the case of  $J=1$  the magnitudes were of similar sizes. Also, the  $\downarrow$  component of the second state of negative energy is now much smaller than the  $\uparrow$  component. The second state has to compensate for the spin flip of the lowest state by increasing the weight of the spin component aligned with the external impurity spin.

In the case of two impurities, the behavior is similar to the case of one impurity, except that now the second state is also

localized. Therefore, for  $J=1$ , there are now two levels at positive energies with only spin  $\uparrow$  contribution and two states at negative energies with only spin  $\downarrow$  contribution. As one crosses to higher values of the coupling, for instance,  $J=2$ , the spin contributions for the bound states change in a similar way to the single impurity case. For the set of parameters, we consider here that the two states are nearly degenerate and therefore the states change their nature basically simultaneously. Otherwise, they would change their nature in succession.<sup>21</sup>

One may also consider a ferromagnetic chain where all the spins point in the  $z$  direction. This case is very similar to the single impurity case, as expected. All the positive energy states have the same spin content at low values of the coupling. If the coupling is large enough, a similar situation will occur where all the bound states have reversed their spin content.

The case of the DW1 is, however, different. Even at a small value of the coupling, in the sense that the first level crossing has not yet occurred, such as  $J=1$ , the various states have a mixture of the two spin components. This is shown in Fig. 19. The bound states at positive energy have a mixture of the two components, even though the magnitude at the impurity site is larger for the  $\uparrow$  component. For the negative energies, the  $\downarrow$  component has a larger magnitude. In Fig. 19, we only show results for the lowest level but a similar trend is found for the other localized states. Note that both components have symmetric wave functions. This does not happen, for instance, for the case of the third level shown in Fig. 20. Even though the relative magnitudes of the spin compo-

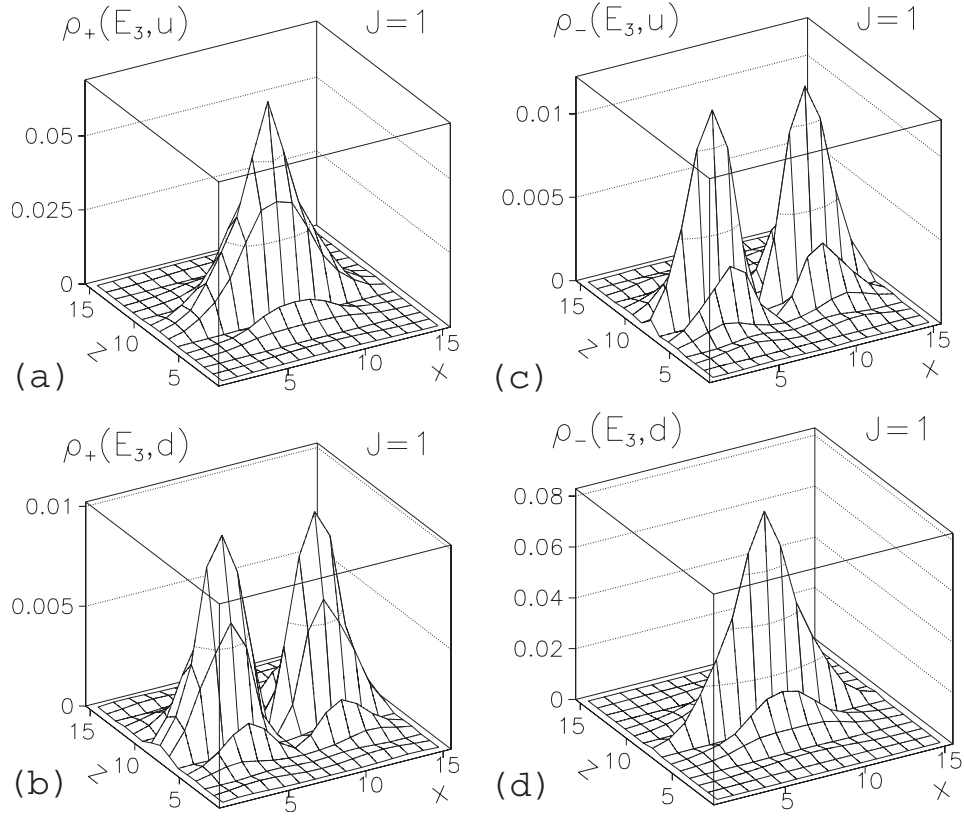


FIG. 20. LDOS for the domain wall DW1. (a)  $\rho_+(\epsilon_3, i, \uparrow)$  for  $J=1$ , (b)  $\rho_+(\epsilon_3, i, \downarrow)$  for  $J=1$ , (c)  $\rho_-(\epsilon_3, i, \uparrow)$  for  $J=1$ , and (d)  $\rho_-(\epsilon_3, i, \downarrow)$  for  $J=1$ . (Note that in the vertical axis, label  $u=\uparrow$  and  $d=\downarrow$ .)

nents are the same, note that while the  $\uparrow$  component has a symmetric wave function, the spin  $\downarrow$  has an antisymmetrical wave function. For the third level at negative energy, this is reversed.

Increasing the coupling to  $J=2$  does not change the nature of the first two level states. However, increasing further to  $J=4$ , we see in Fig. 21 that there is once again a reversal of the magnitudes of the two spin components of the first level. Even though both spin components contribute, the magnitude of the  $\downarrow$  component is now larger than the magnitude of the  $\uparrow$  component. This also occurs for the second level. For the third level, however, the two components have very similar magnitudes.

As we have seen in some cases, the discrete states in the gap correspond to well defined spin polarized states. Then, the QPT changes the spin polarization of these states, leading to a sort of magnetic phase transition. However, in the case of the DW1 domain wall, each discrete level corresponds to a mixture of spin up and down components because the spins in DW are oriented along the  $x$  axis. In this case, the QPT does not show explicitly the transition between spin up and down states. Nevertheless, the different spin components of the composition are also interchanged during the QPT. Thus, the analysis demonstrates that the QPT can be seen in the variation of magnetic state corresponding to the discrete levels. As for the origin of the QPT, we show that it is related only to the level crossing because at each crossing point the ground state is reconstructed.

### C. Kinetic energy

To further confirm the nature of the states, we have calculated at  $T=0$ ,

$$\langle c_{i\sigma}^\dagger c_{j\sigma'} \rangle = \sum_n \sigma \sigma' v_n(i, \sigma) v_n(j, \sigma'). \quad (18)$$

We have considered two typical points in the system: the central point and a point far from the central line (in the bulk). Also, we have considered both vertical (v) (along  $z$ ) and horizontal (h) (along  $x$ ) displacements of the electrons. In Figs. 22 and 23, we plot the hoppings for the cases of  $\sigma, \sigma' = \uparrow$  and  $\sigma, \sigma' = \downarrow$  as a function of the coupling. We have considered the cases of a single impurity, two impurities (four lattice sites apart), the domain wall DW1, and a ferromagnetic chain. In the bulk, we expect the states to be extended independently of the coupling. This is so and the hoppings are basically independent of  $J$  both along the vertical and horizontal directions and spin directions. The central point is different, however, and when various impurity spins are considered, the horizontal and vertical directions are expected to be different. As shown in Figs. 22 and 23, we see that as the coupling grows, in general, the hopping decreases, consistently with the “localized” nature of the states. This is particularly so along the chain direction, for the lines of spins. In the case of two impurities, and due to the rather local nature of the effect of the impurity spins, the hoppings at the central point do not change much as a function of the



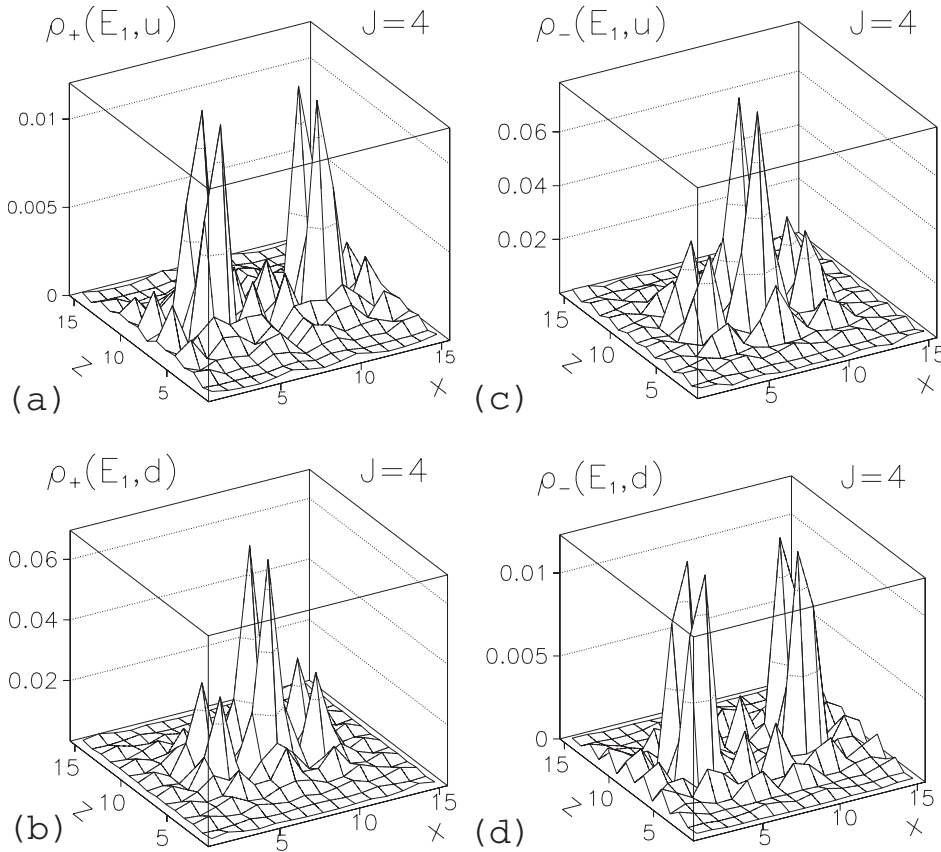


FIG. 21. LDOS for the domain wall DW1. (a)  $\rho_+(\epsilon_1, i, \uparrow)$  for  $J=4$ , (b)  $\rho_+(\epsilon_1, i, \downarrow)$  for  $J=4$ , (c)  $\rho_-(\epsilon_1, i, \uparrow)$  for  $J=4$ , and (d)  $\rho_-(\epsilon_1, i, \downarrow)$  for  $J=4$ . (Note that in the vertical axis, label  $u=\uparrow$  and  $d=\downarrow$ .)

coupling. As the  $\uparrow$  spins are in majority, the hopping term for the cases of  $\uparrow, \uparrow$  are typically larger. Interestingly, and even though the hopping term of the Hamiltonian is diagonal in the spin, in the case of the domain wall DW1, there is a nonvanishing spin flip term, even though quite small.

## V. STABILITY OF DOMAIN WALL

So far, we have assumed that the domain wall is stable. We may solve this stability issue self-consistently and study the stability of the domain wall. This may be achieved by introducing effective interactions between the impurity spins, possibly mediated by the quasiparticles. Let us approximate these interactions by an Heisenberg-like term. The part of the Hamiltonian involving the classical spins may be written in mean field as

$$-\sum_i J(S_i^x \langle \sigma^x \rangle_i + S_i^z \langle \sigma^z \rangle_i) - \frac{1}{2} \sum_{\langle i,j \rangle} J_f (S_i^x S_j^x + S_i^z S_j^z), \quad (19)$$

where we consider only the coupling between nearest neighbors, assumed to be ferromagnetic for simplicity. In the mean-field approximation for both electrons and spins, the external impurity spins are determined from their mutual interactions and the interaction with the average spin density of the electrons. We look for the equilibrium impurity spin configuration minimizing the energy with respect to the impurity

spin components. This equilibrium distribution is then inserted in the Bogoliubov–de Gennes equations and solved self-consistently. The impurity spins satisfy the constraint that  $(S_i^x)^2 + (S_i^z)^2 = (\tilde{S}_i)^2$ . An equivalent way is to minimize the Hamiltonian with respect to the angles themselves, since in this way the constraint is automatically enforced. Minimizing with respect to the angles  $\varphi_i$ , we get the set of equations

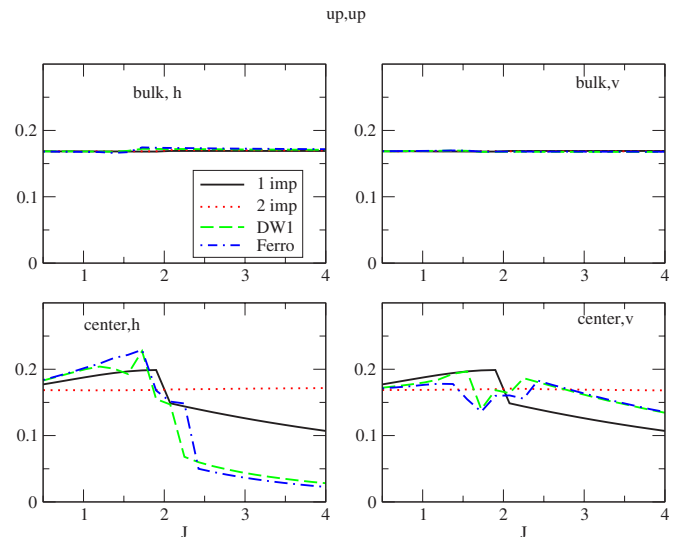


FIG. 22. (Color online) Hopping matrix elements for up spin electrons from a bulk point and the center point, in the horizontal (along  $x$ ) and vertical (along  $z$ ) directions.

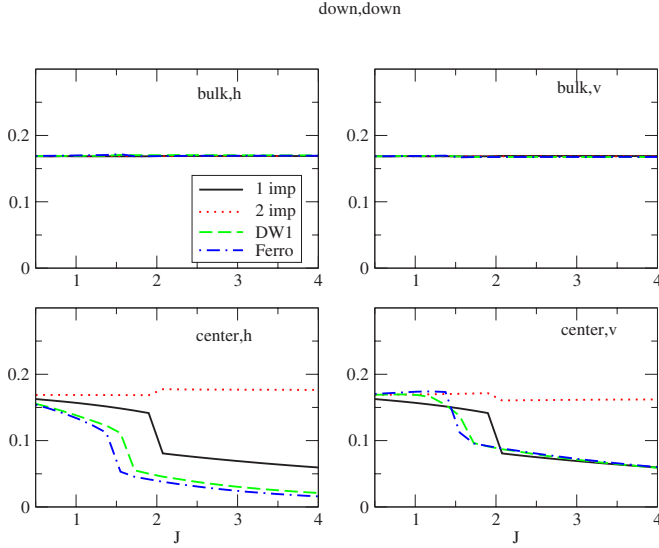


FIG. 23. (Color online) Hopping matrix elements for down spin electrons from a bulk point and the center point, in the horizontal (along  $x$ ) and vertical (along  $z$ ) directions.

$$\begin{aligned}
 & -J\langle\sigma^z\rangle_i \cos \varphi_i + J\langle\sigma^x\rangle_i \sin \varphi_i + J_f \sin \varphi_i \cos \varphi_{i+\delta} \\
 & -J_f \cos \varphi_i \sin \varphi_{i+\delta} = 0,
 \end{aligned} \quad (20)$$

where  $\delta = \pm 1$ . These equations hold at each impurity site. The solution leads to a stable domain wall whose shape depends on  $\frac{J}{J_f}$ . The results are shown in Fig. 24. We see that the profiles are stable. In the case of a small coupling between the impurity spins ( $J_f = 0.1$ ), for small  $J$  the profile is tending to a large  $\lambda$ , defined in Eqs. (14) and (15), which implies an almost linear profile between the end spins. As  $J$  increases, the value of  $\lambda$  decreases and there seems to be a rapid variation between  $J=1$  and  $J=2$ . Increasing the value of  $J_f$ , the stability is improved. For large  $J_f$ , the profile is almost independent of  $J$ . Also note that by increasing  $J_f$ , the value of  $\lambda$  increases and the profile becomes almost linear for any value of  $J$ .

We should note that one strictly does not have to introduce an effective Heisenberg interaction between the impurity spins, if we were to treat them as quantum mechanical. The Kondo interaction would couple the impurity spins to the conduction electron spin density, which in turn would give rise dynamically to an effective long-range interaction between the impurity spins. In our mean-field approach, this interaction is introduced phenomenologically, much in the same way as the attractive interaction between the electrons to give rise to pairing. While a mean-field approach (BCS) is quite good for the superconductivity order, the correct description of the Kondo effect is much more involved as well as a proper treatment of the coupling between the impurity spins. However, as shown before in a similar context,<sup>69</sup> the results are quite similar.

## VI. EFFECT OF TEMPERATURE

In this section, we briefly study the effect of temperature on the results. Clearly, the quantum phase transitions are smeared out but the same trends prevail.

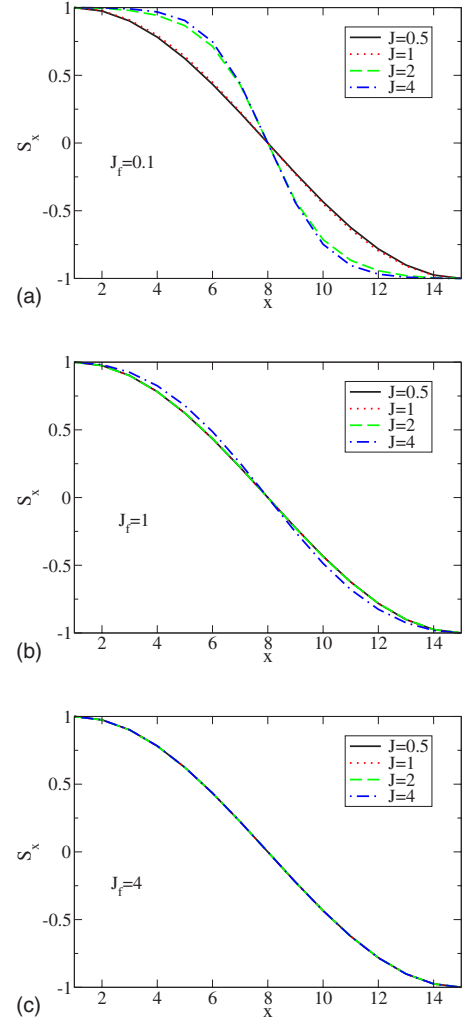


FIG. 24. (Color online) Profile of  $S_x$  of the impurity spins for DW1 and for for  $J_f = 0.1, 1, 4$  as a function of  $J$ .

In Fig. 25, we show the order parameter and the spin density for a single impurity and the DW1 as a function of temperature for the two typical cases of  $J=1, 2$ . We clearly see that the critical temperature is basically the same when we increase the number of spins. Note the critical temperature for one impurity and the DW1 at about  $T \sim 0.5-0.6$ . However, the behavior of the spin density is quite different as a result of the underlying phase transition. In the case of  $J=2$ , the spin density is finite and then decreases, while for  $J=1$  the increase in temperature increases the density due to excitation to higher levels. Note for both cases the different starting point of  $s_z^T$  due to the quantum phase transition when we go from  $J=1$  to  $J=2$ .

Clearly, as shown in Fig. 26, the quantum transitions between the plateaus of the spin densities as a function of the coupling are now smeared, but the same overall trend persists. Even though the temperature smoothens the curves and the quantum phase transitions disappear (they only occur at  $T=0$ ), the behaviors are robust to temperature. In particular, the regimes where at  $T=0$  there is a finite value for one of the average magnetizations, it persists at small finite temperatures.

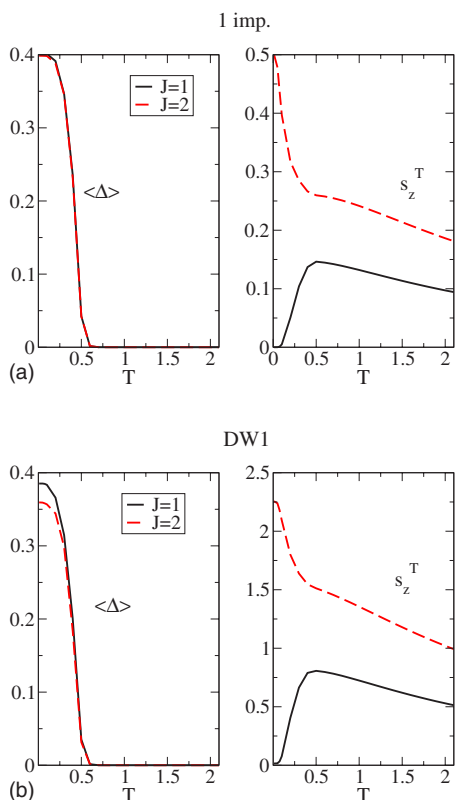


FIG. 25. (Color online)  $\langle \Delta \rangle$  and  $s_z^T$  for one impurity and DW1 as a function of temperature for various values of  $J$ .

## VII. SUMMARY

In this work we considered the effect of correlated magnetic impurities inserted in a conventional superconductor. Previous results on few impurities revealed the existence of sequences of quantum phase transitions, associated with level crossings, that lead to discontinuous changes in the properties of the system, such as the magnetization. We extended these results to the case when we have sets of impurity spins that are correlated through mutual interactions that may be originated via RKKY-type interactions mediated by the electrons. In particular, we considered cases where the impurity spins are organized in such a way that form domain walls which, to simplify, we have limited in this work to one-dimensional arrays of spins inserted in the superconductor. These domain wall structures may be obtained by imposing different boundary conditions at different sides of the mesoscopic systems considered here. As in the case of a few impurities, we found a series of quantum phase transitions that we have analyzed. In general, the introduction of

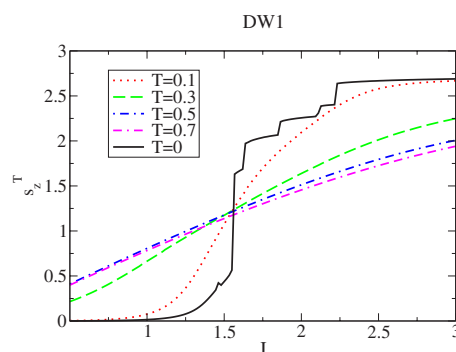


FIG. 26. (Color online) Effect of temperature on the results for the various magnetizations (total and left or right) for DW1.

foreign objects in the superconductor originates interference effects. These are revealed in the LDOS. We have presented detailed results which show the complex nature of the multiple interference effects.

We have also shown that the domain wall structures considered here are stable, taking into account the mediated interactions between the impurity spins. To simplify, we considered in this work classical spins. The case of a full quantum problem where the impurity spins are described by quantum operators leads to Kondo-like effects in the superconductor. This is much more involved and the use of the Bogoliubov–de Gennes formalism requires that we take this classical limit. Fortunately, at least if the coupling between the electronic spin density and the impurity spins is not large, the classical description is enough.

In this work, we focused on the effect of the impurity spins on the superconductor. The opposite problem of the effect of the superconductor on the impurity spins may be interesting if, for instance, by passing a current through the superconductor, the spin torque created by a spin polarized current on the impurity spins changes their relative orientations. This is a problem that has received much attention in the context of spintronics, where spin polarized currents passing through a magnetic semiconductor move the position of the domain walls. The related problem in the context of the magnetic correlated impurity spins in the superconductor will be considered elsewhere.

## ACKNOWLEDGMENTS

This work is supported by FCT Grant No. POCI/FIS/58746/2004 in Portugal, the ESF Science Programme INSTANS 2005-2010, Polish Ministry of Science and Higher Education as a research project in years 2006–2009, and by STCU Grant No. 3098 in Ukraine.

<sup>1</sup>A. V. Balatsky, and I. Vekhter and J.-X. Zhu, *Rev. Mod. Phys.* **78**, 373 (2006).

<sup>2</sup>P. W. Anderson, *Phys. Rev. Lett.* **3**, 325 (1959).

<sup>3</sup>K. Ueda and T. M. Rice, in *Theory of Heavy Fermions and Va-*

*lence Fluctuations*, edited by T. Kasuya and T. Saso (Springer, Berlin, 1985).

<sup>4</sup>P. A. Lee, *Phys. Rev. Lett.* **71**, 1887 (1993); Y. Hatsugai and P. A. Lee, *Phys. Rev. B* **48**, 4204 (1993).

- <sup>5</sup>M. Franz, C. Kallin, and A. J. Berlinsky, Phys. Rev. B **54**, R6897 (1996); M. Franz, C. Kallin, A. J. Berlinsky, and M. I. Salkola, *ibid.* **56**, 7882 (1997).
- <sup>6</sup>S. Haas, A. V. Balatsky, M. Sigrist, and T. M. Rice, Phys. Rev. B **56**, 5108 (1997).
- <sup>7</sup>A. Altland, B. D. Simons, and M. R. Zirnbauer, Phys. Rep. **359**, 283 (2002).
- <sup>8</sup>A. A. Nersisyan, A. M. Tsvetik, and F. Wenger, Phys. Rev. Lett. **72**, 2628 (1994); Nucl. Phys. B **438**, 561 (1995).
- <sup>9</sup>T. Senthil, M. P. A. Fisher, L. Balents, and C. Nayak, Phys. Rev. Lett. **81**, 4704 (1998).
- <sup>10</sup>W. A. Atkinson, P. J. Hirschfeld, and A. H. MacDonald, Phys. Rev. Lett. **85**, 3922 (2000).
- <sup>11</sup>A. Ghosal, M. Randeria, and N. Trivedi, Phys. Rev. B **63**, 020505(R) (2000).
- <sup>12</sup>E. R. Ulm, J. T. Kim, T. R. Lemberger, S. R. Foltyn, and X. Wu, Phys. Rev. B **51**, 9193 (1995); D. N. Basov, A. V. Puchkov, R. A. Hughes, T. Strach, J. Preston, T. Timusk, D. A. Bonn, R. Liang, and W. N. Hardy, *ibid.* **49**, 12165 (1994); C. Bernhard, J. L. Tallon, C. Bucci, R. De Renzi, G. Guidi, G. V. M. Williams, and C. Niedermayer, Phys. Rev. Lett. **77**, 2304 (1996); S. H. Moffat, R. A. Hughes, and J. S. Preston, Phys. Rev. B **55**, R14741 (1997).
- <sup>13</sup>A. Ghosal, M. Randeria, and N. Trivedi, Phys. Rev. Lett. **81**, 3940 (1998).
- <sup>14</sup>A. A. Abrikosov and L. P. Gor'kov, Zh. Eksp. Teor. Fiz. **39**, 178 (1960) [Sov. Phys. JETP **12**, 1243 (1961)].
- <sup>15</sup>R. Ramazashvili and P. Coleman, Phys. Rev. Lett. **79**, 3752 (1997).
- <sup>16</sup>A. Sakurai, Prog. Theor. Phys. **44**, 1472 (1970).
- <sup>17</sup>K. Satori, H. Shiba, O. Sakai, and Y. Shimizu, J. Phys. Soc. Jpn. **61**, 3239 (1992).
- <sup>18</sup>A. C. Hewson, *The Kondo Effect to Heavy Fermions* (Cambridge University Press, Cambridge, 1993).
- <sup>19</sup>M. I. Salkola, A. V. Balatsky, and J. R. Schrieffer, Phys. Rev. B **55**, 12648 (1997).
- <sup>20</sup>D. K. Morr and N. A. Stavropoulos, Phys. Rev. B **67**, 020502(R) (2003).
- <sup>21</sup>D. K. Morr and J. Yoon, Phys. Rev. B **73**, 224511 (2006).
- <sup>22</sup>H. C. Manoharan, C. P. Lutz, and D. M. Eigler, Nature (London) **403**, 512 (2000).
- <sup>23</sup>V. S. Stepanyuk, L. Niebergall, W. Hergert, and P. Bruno, Phys. Rev. Lett. **94**, 187201 (2005).
- <sup>24</sup>T. Pereg-Barnea and M. Franz, Int. J. Mod. Phys. B **19**, 731 (2005).
- <sup>25</sup>D. K. Morr and N. A. Stavropoulos, Phys. Rev. Lett. **92**, 107006 (2004).
- <sup>26</sup>A. I. Larkin, V. I. Melnikov, and D. E. Khmel'nitskii, Zh. Eksp. Teor. Fiz. **60**, 846 (1971) [Sov. Phys. JETP **33**, 458 (1971)].
- <sup>27</sup>V. M. Galitski and A. I. Larkin, Phys. Rev. B **66**, 064526 (2002).
- <sup>28</sup>A. A. Abrikosov, *Fundamentals of the Theory of Metals* (Elsevier, Amsterdam, 1988).
- <sup>29</sup>D. N. Aristov, S. V. Maleyev, and A. G. Yashechkin, Z. Phys. B: Condens. Matter **102**, 467 (1997).
- <sup>30</sup>L. N. Bulaevskii, A. I. Buzdin, M. I. Kulić, and S. V. Panyukov, Adv. Phys. **34**, 175 (1985).
- <sup>31</sup>N. D. Mathur, F. M. Grosche, S. R. Julian, I. R. Walker, D. Freye, R. Haselwimmer, and G. Lonzarich, Science **394**, 39 (1998).
- <sup>32</sup>M. B. Maple, arXiv:cond-mat/9802202 (unpublished).
- <sup>33</sup>C. Bourbonnais and D. Jérôme, Science **281**, 1155 (1998).
- <sup>34</sup>K. Ishida, Y. Kawasaki, K. Tabuchi, K. Kashima, Y. Kitaoka, K. Asayama, C. Geibel, and F. Steglich, Phys. Rev. Lett. **82**, 5353 (1999).
- <sup>35</sup>R. Caspary, P. Hellmann, M. Keller, G. Sparn, C. Wassilew, R. Köhler, C. Geibel, C. Schank, F. Steglich, and N. E. Phillips, Phys. Rev. Lett. **71**, 2146 (1993).
- <sup>36</sup>R. Feyerherm, A. Amato, F. N. Gygax, A. Schenck, C. Geibel, F. Steglich, N. Sato, and T. Komatsubara, Phys. Rev. Lett. **73**, 1849 (1994).
- <sup>37</sup>N. Bernhoeft, N. Sato, B. Roessli, N. Aso, A. Hiess, G. H. Lander, Y. Endoh, and T. Komatsubara, Phys. Rev. Lett. **81**, 4244 (1998).
- <sup>38</sup>N. Aso, B. Roessli, N. Bernhoeft, R. Calemczuk, N. K. Sato, Y. Endoh, T. Komatsubara, A. Hiess, G. H. Lander, and H. Kad-owaki, Phys. Rev. B **61**, R11867 (2000).
- <sup>39</sup>M. A. N. Araújo, N. M. R. Peres, and P. D. Sacramento, Phys. Rev. B **65**, 012503 (2001).
- <sup>40</sup>P. D. Sacramento, J. Phys.: Condens. Matter **15**, 6285 (2003).
- <sup>41</sup>M. Lange, M. J. Van Bael, Y. Bruynseraede, and V. V. Moshchalkov, Phys. Rev. Lett. **90**, 197006 (2003).
- <sup>42</sup>D. Stamopoulos, M. Pissas, and E. Manios, Phys. Rev. B **71**, 014522 (2005).
- <sup>43</sup>Z. Yang, M. Lange, A. Volodin, R. Szymczak, and V. V. Moshchalkov, Nat. Mater. **3**, 793 (2004).
- <sup>44</sup>W. Gillijns, A. Yu. Aladyshkin, M. Lange, M. J. Van Bael, and V. V. Moshchalkov, Phys. Rev. Lett. **95**, 227003 (2005).
- <sup>45</sup>A. I. Buzdin, Rev. Mod. Phys. **77**, 935 (2005).
- <sup>46</sup>I. F. Lyuksyutov and V. L. Pokrovsky, Adv. Phys. **54**, 67 (2005).
- <sup>47</sup>F. S. Bergeret, A. F. Volkov, and K. B. Efetov, Rev. Mod. Phys. **77**, 1321 (2005).
- <sup>48</sup>M. V. Milosevic and F. M. Peeters, J. Low Temp. Phys. **139**, 257 (2005).
- <sup>49</sup>K. Halterman and O. T. Valls, Phys. Rev. B **65**, 014509 (2001).
- <sup>50</sup>V. Shelukhin, A. Tsukernik, M. Karpovskii, Y. Blum, K. B. Efetov, A. F. Volkov, T. Champel, M. Eschrig, T. Lofwander, G. Schon, and A. Palevski, Phys. Rev. B **73**, 174506 (2006).
- <sup>51</sup>M. Yu. Kharitonov, A. F. Volkov, and K. B. Efetov, Phys. Rev. B **73**, 054511 (2006).
- <sup>52</sup>I. F. Lyuksyutov and V. L. Pokrovsky, Phys. Rev. Lett. **81**, 2344 (1998).
- <sup>53</sup>I. F. Lyuksyutov and D. G. Naugle, Mod. Phys. Lett. B **13**, 491 (1999).
- <sup>54</sup>I. F. Lyuksyutov and V. L. Pokrovsky, Mod. Phys. Lett. B **14**, 409 (2000).
- <sup>55</sup>M. Cardoso, P. Bicudo, and P. D. Sacramento, J. Phys.: Condens. Matter **18**, 8623 (2006).
- <sup>56</sup>M. Cardoso, P. Bicudo, and P. D. Sacramento, Ann. Phys. (N.Y.) (to be published).
- <sup>57</sup>I. Žutić, J. Fabian, and S. Das Sarma, Rev. Mod. Phys. **76**, 323 (2004).
- <sup>58</sup>S. A. Wolf, D. D. Awschalom, R. A. Buhrman, J. M. Daughton, S. von Molnár, M. L. Roukes, A. Y. Chtchelkanova, and D. M. Treger, Science **294**, 1488 (2001).
- <sup>59</sup>C. Rüster, T. Borzenko, C. Gould, G. Schmidt, L. W. Molenkamp, X. Liu, T. J. Wojtowicz, J. K. Furdyna, Z. G. Yu, and M. E. Flatté, Phys. Rev. Lett. **91**, 216602 (2003).
- <sup>60</sup>T. Dietl, H. Ohno, and F. Matsukura, Phys. Rev. B **63**, 195205 (2001).
- <sup>61</sup>H. Ohno, D. Chiba, F. Matsukura, T. O. E. Abe, T. Dietl, Y. Ohno, and K. Ohtani, Nature (London) **408**, 944 (2000).

- <sup>62</sup>T. Dietl, H. Ohno, F. Matsukura, J. Cibert, and D. Ferrand, *Science* **287**, 1019 (2000).
- <sup>63</sup>S. Maekawa, S. Takahashi, and H. Imamura, in *Spin Dependent Transport in Magnetic Nanostructures*, edited by S. Maekawa and T. Shinjo (Taylor & Francis, London, 2002), p. 143.
- <sup>64</sup>S. Takahashi, H. Imamura, and S. Maekawa, *Phys. Rev. Lett.* **82**, 3911 (1999).
- <sup>65</sup>J.-X. Zhu and C. S. Ting, *Phys. Rev. B* **61**, 1456 (2000).
- <sup>66</sup>M. Berciu, T. G. Rappoport, and B. Janko, *Nature (London)* **435**, 71 (2005).
- <sup>67</sup>P. G. de Gennes, *Superconductivity of Metals and Alloys* (Addison-Wesley, Reading, MA, 1989).
- <sup>68</sup>P. Schlottmann, *Phys. Rev. B* **13**, 1 (1976).
- <sup>69</sup>P. Schlottmann, *Solid State Commun.* **16**, 1297 (1975).